Electronic Supplementary Material (ESI) for Journal of Materials Chemistry C.
This journal is © The Royal Society of Chemistry 2024

Electronic supplementary information

Smart Emissive Hybrid Dynamer and Nanocomposite Made of Complementary Organic and Inorganic Emitters Combined *via* a Supramolecular Janus Synthon

Ilya V. Kashnik,[a,b] Jeanne Rebours,[a] Noée Dumait,[a] Konstantin A. Brylev,[b] and Yann Molard*[,a]

[a] I. V. Kashnik, Jeanne Rebours, Noée Dumait, Pr. Yann Molard
Université de Rennes, CNRS, ISCR – UMR 6226, ScanMAT – UAR 2025, Rennes F-35000, France
E-mail: yann.molard@univ-rennes.fr

[b] I. V. Kashnik, Pr. K.A. Brylev
Nikolaev Institute of Inorganic Chemistry SB RAS, 3 Acad. Lavrentiev ave., 630090 Novosibirsk, Russian Federation

Table of contents

1. NMR spectra

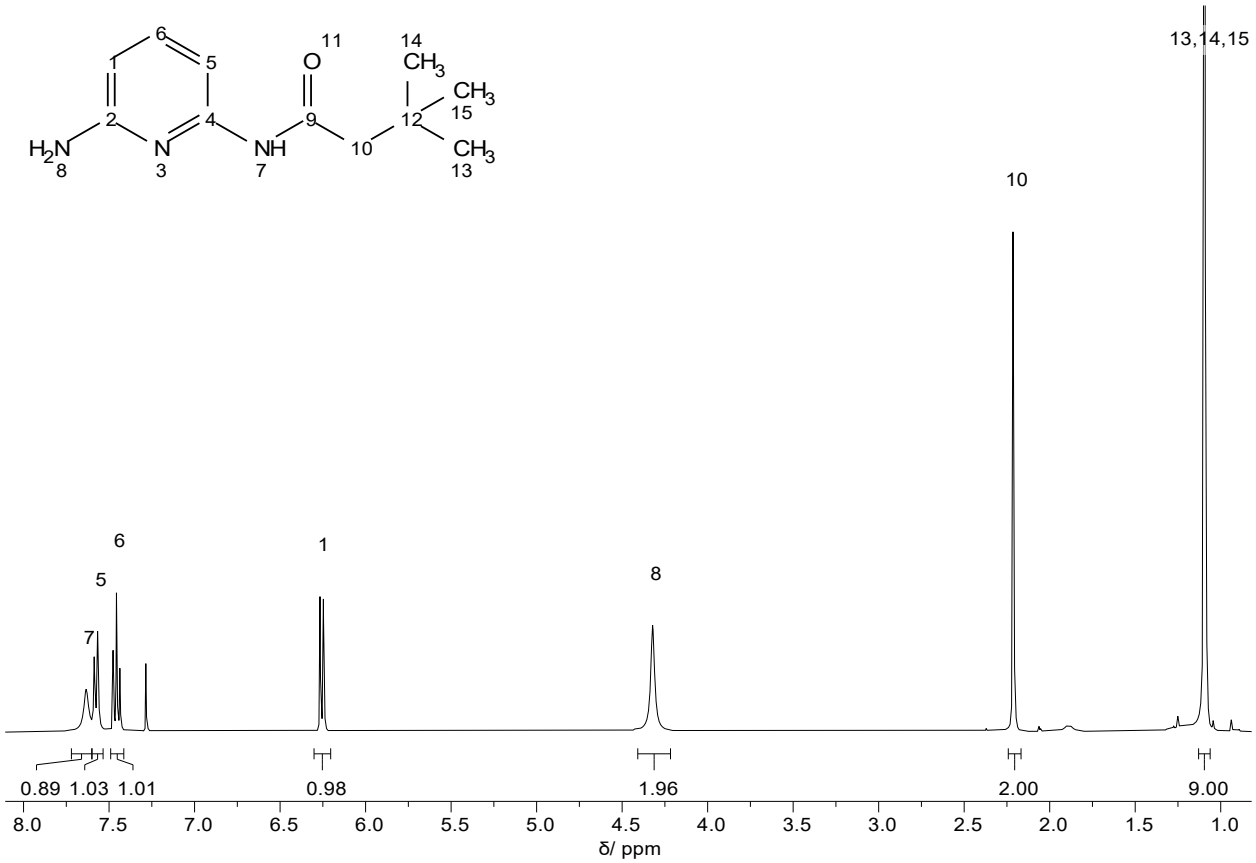

Figure S1. 400 MHz ^{1}H NMR spectrum in $CDCl_3$ of **2**

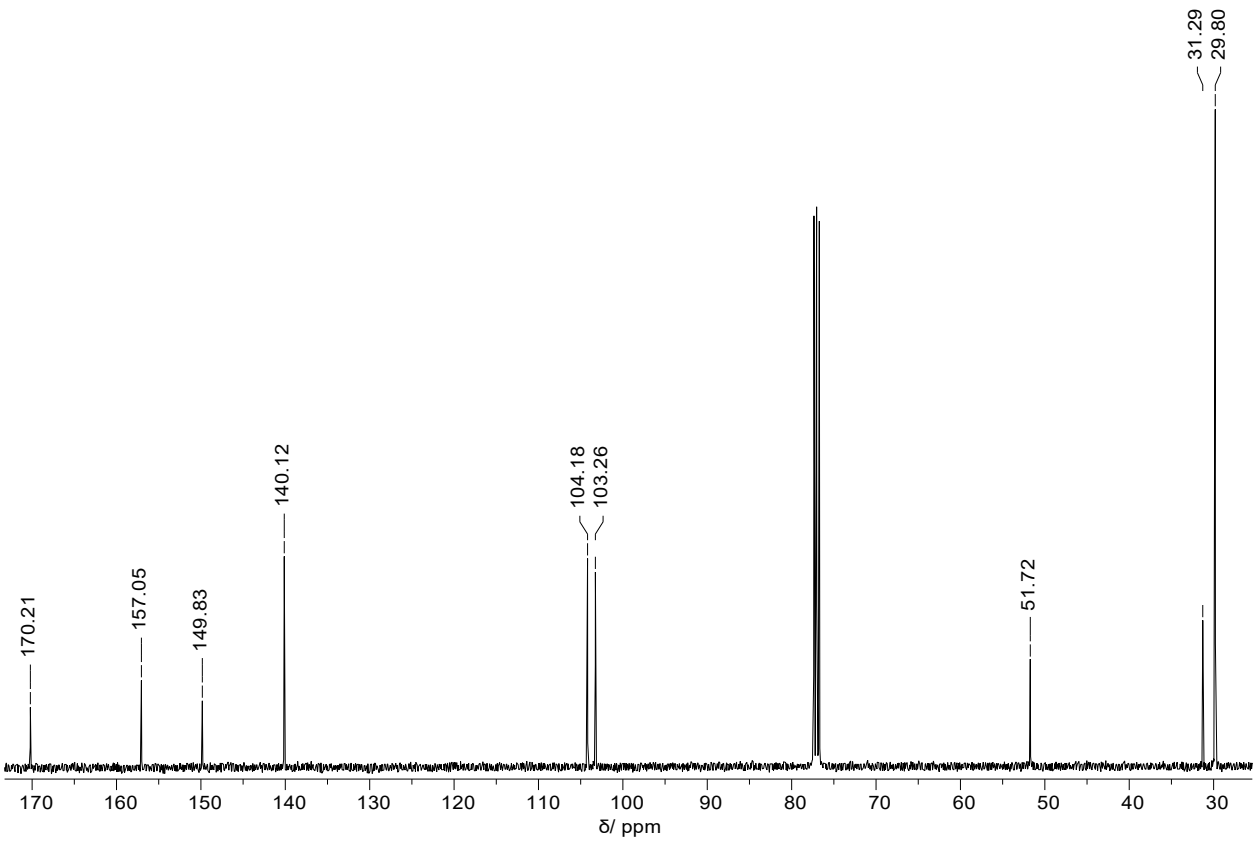

Figure S2. 101 MHz ^{13}C NMR spectrum in $CDCl_3$ of **2**

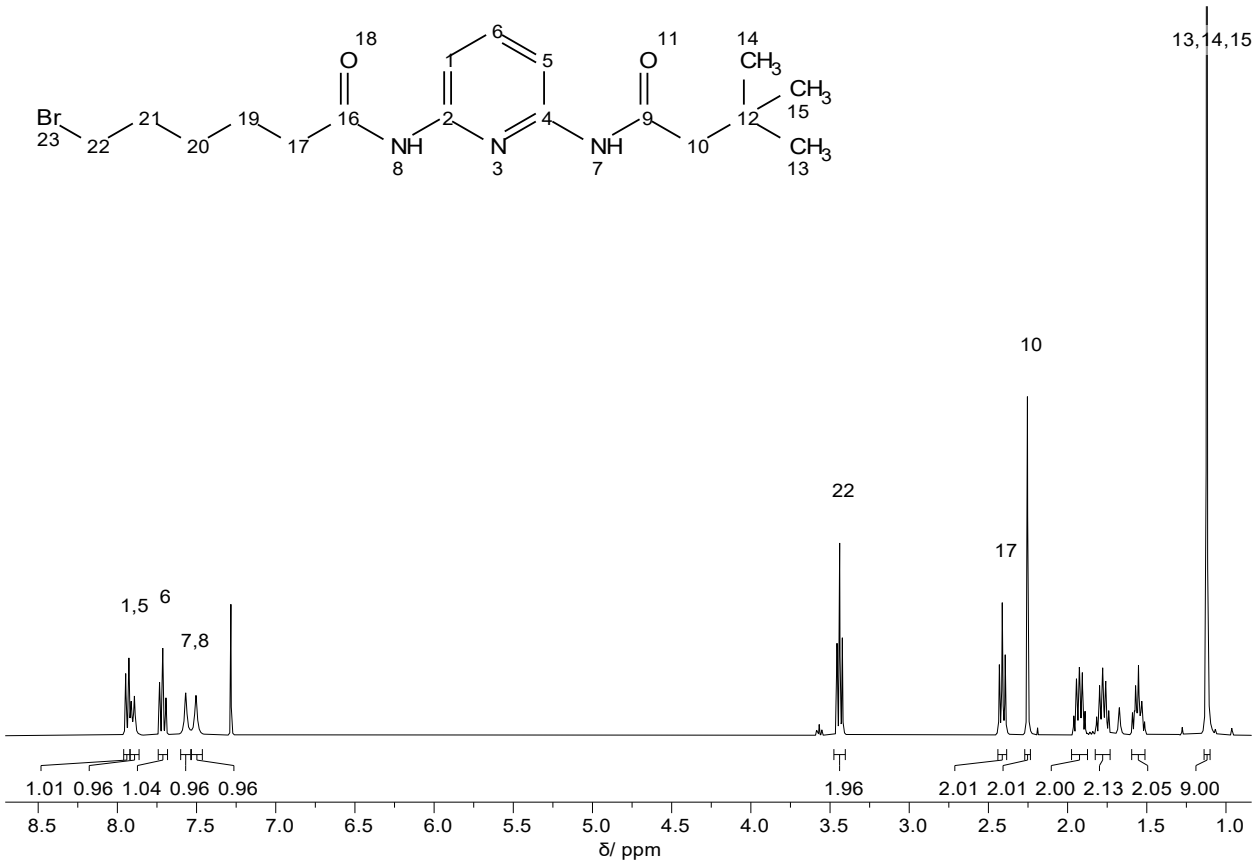

Figure S3. 400 MHz ^{1}H NMR spectrum in $CDCl_3$ of **3**

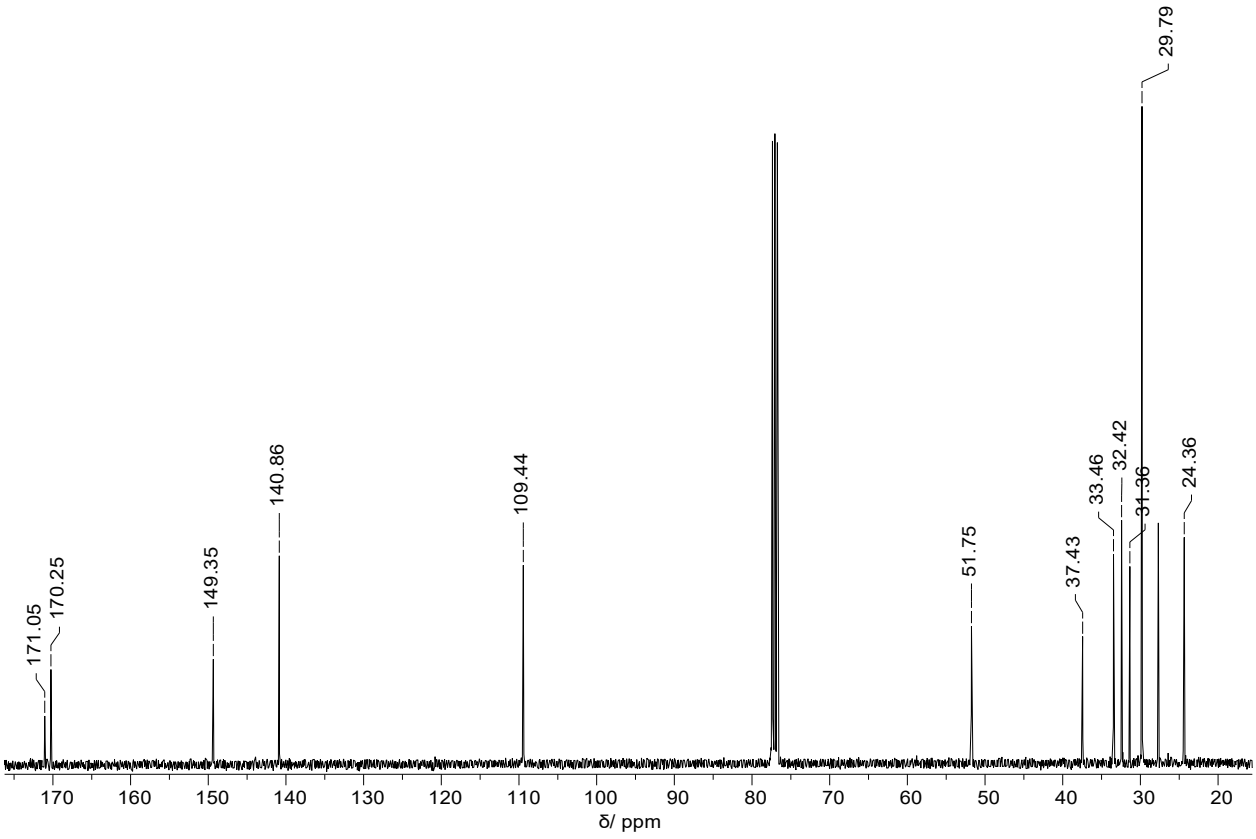

Figure S4. 101 MHz ^{13}C NMR spectrum in $CDCl_3$ of **3**

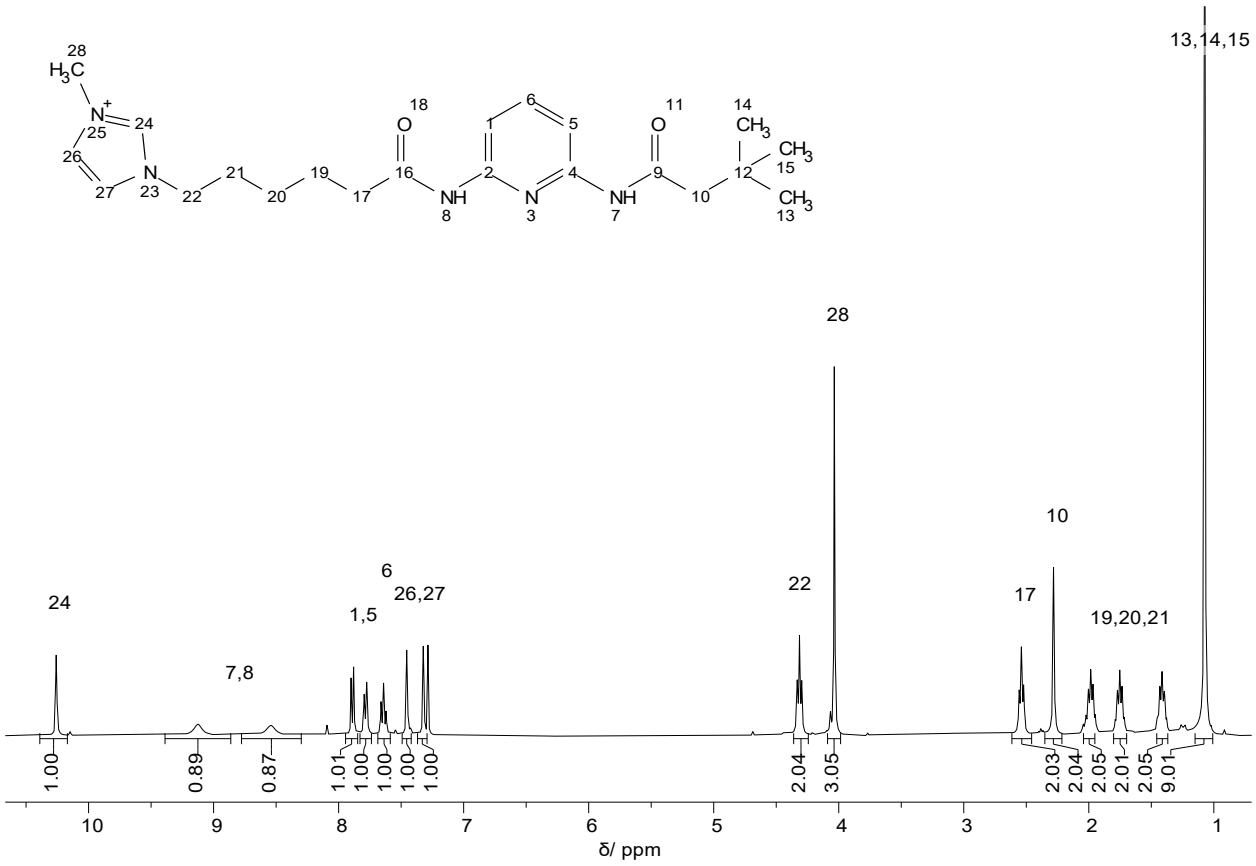

Figure S5. 400 MHz ^{1}H NMR spectrum in $CDCl_3$ of **DAPImBr**

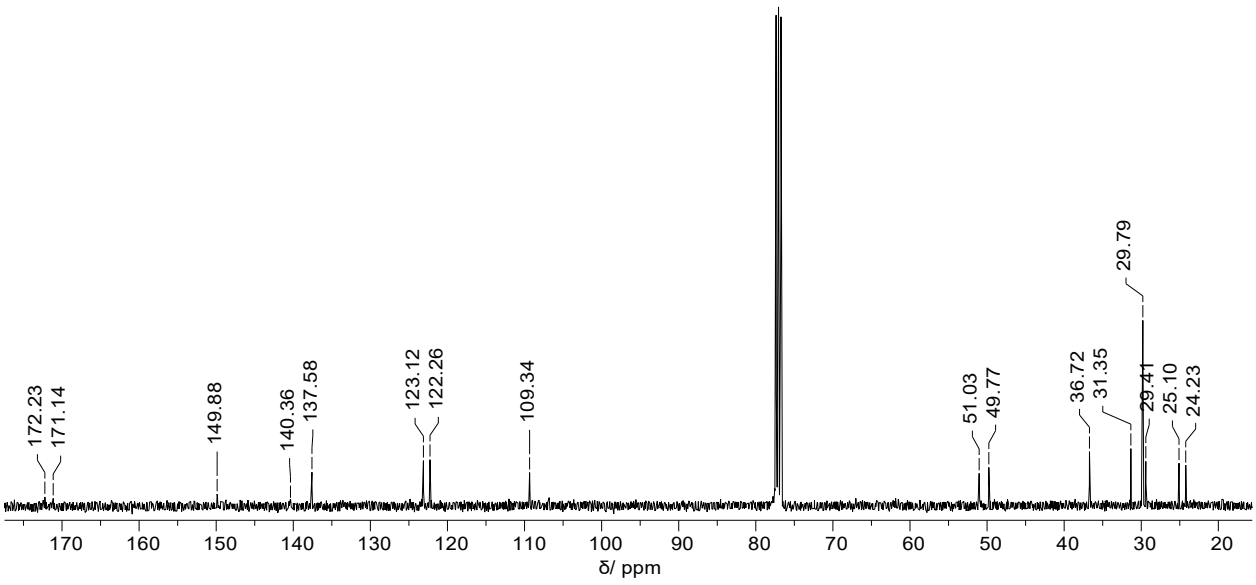

Figure S6. 101 MHz ^{13}C NMR spectrum in $CDCl_3$ of **DAPImBr**

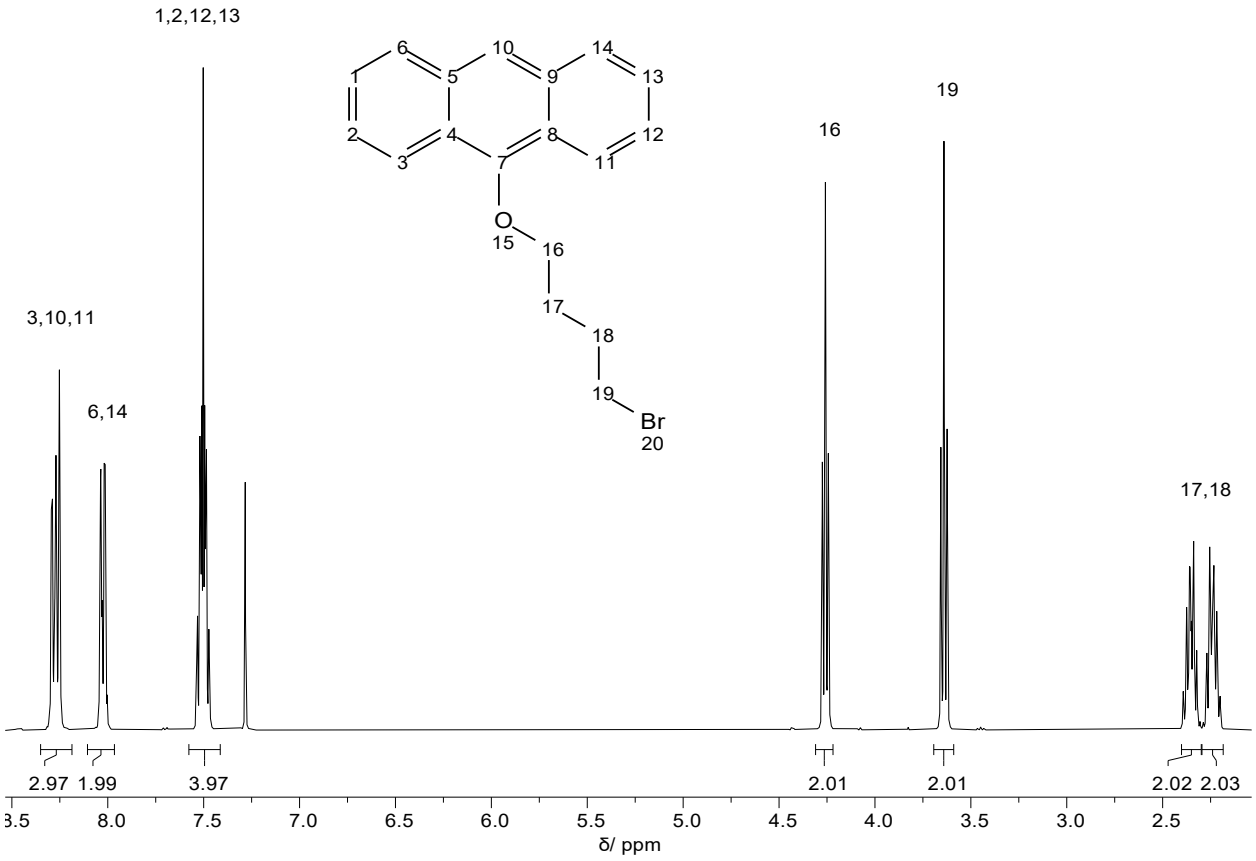

Figure S7. 400 MHz ^{1}H NMR spectrum in $CDCl_3$ of **5**

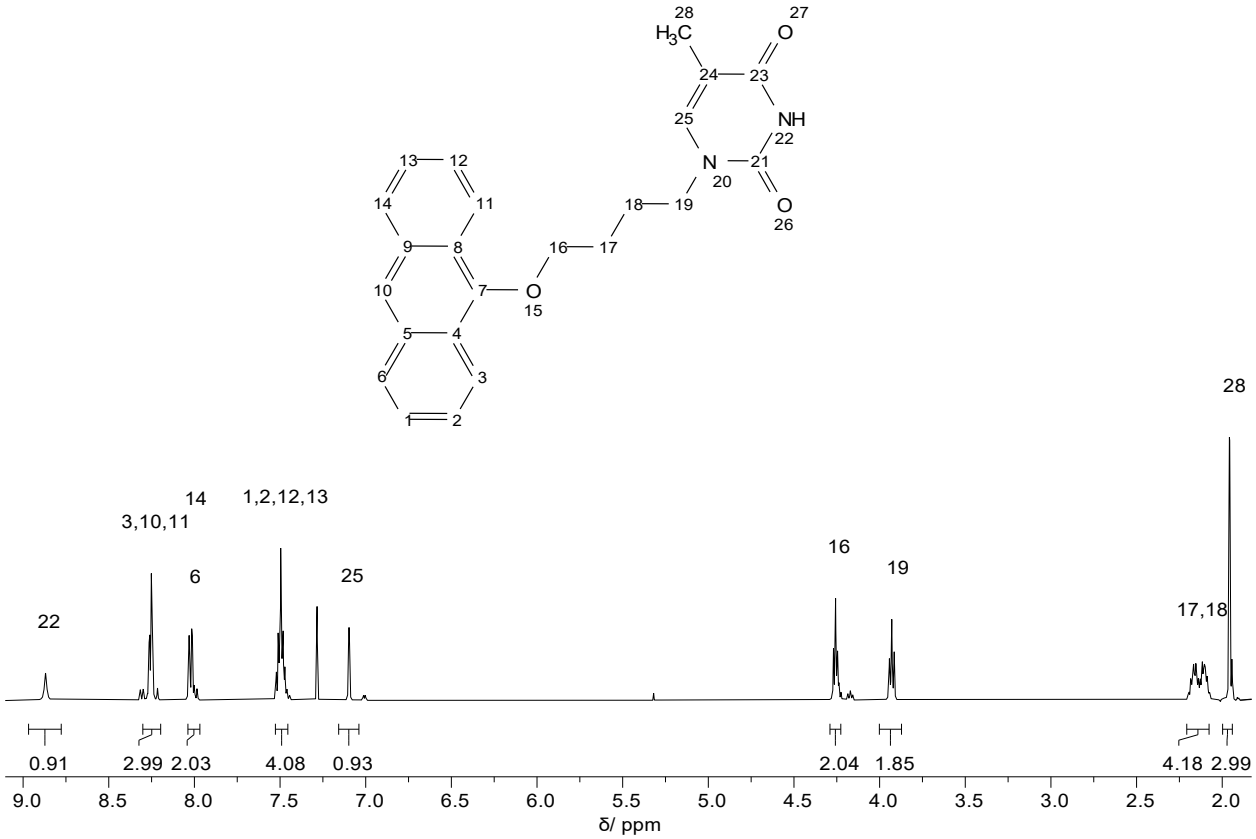

Figure S8. 500 MHz ^{1}H NMR spectrum in $CDCl_3$ of **An-Th**

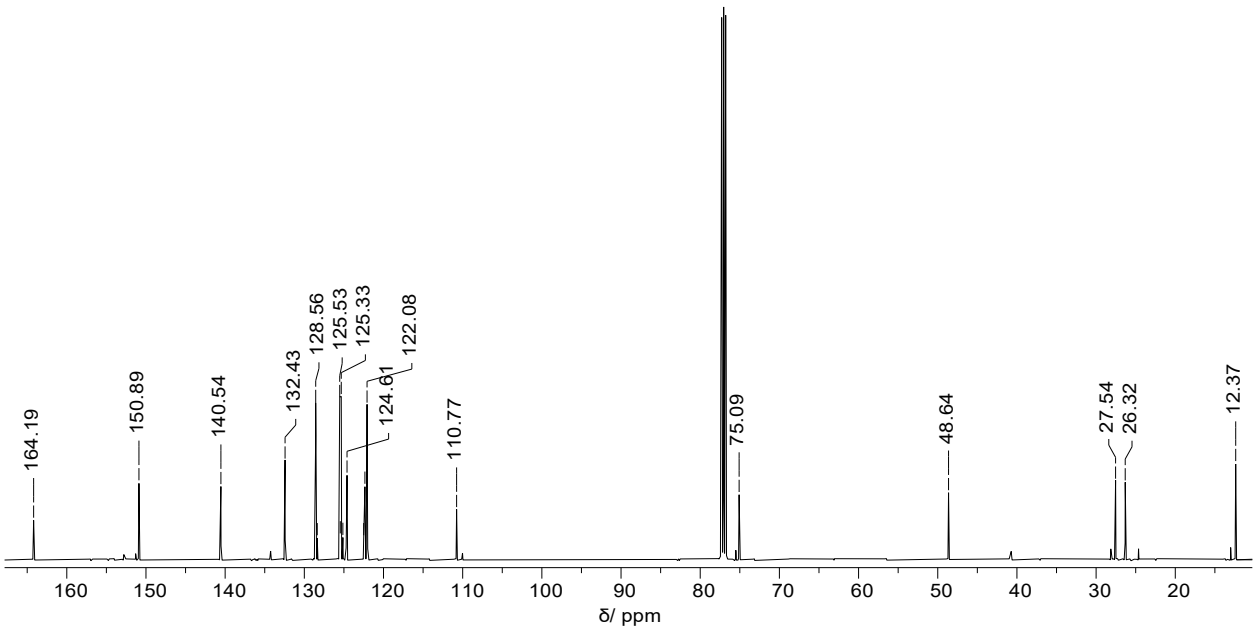

Figure S9. 126 MHz ^{13}C NMR spectrum in $CDCl_3$ of **An-Th**

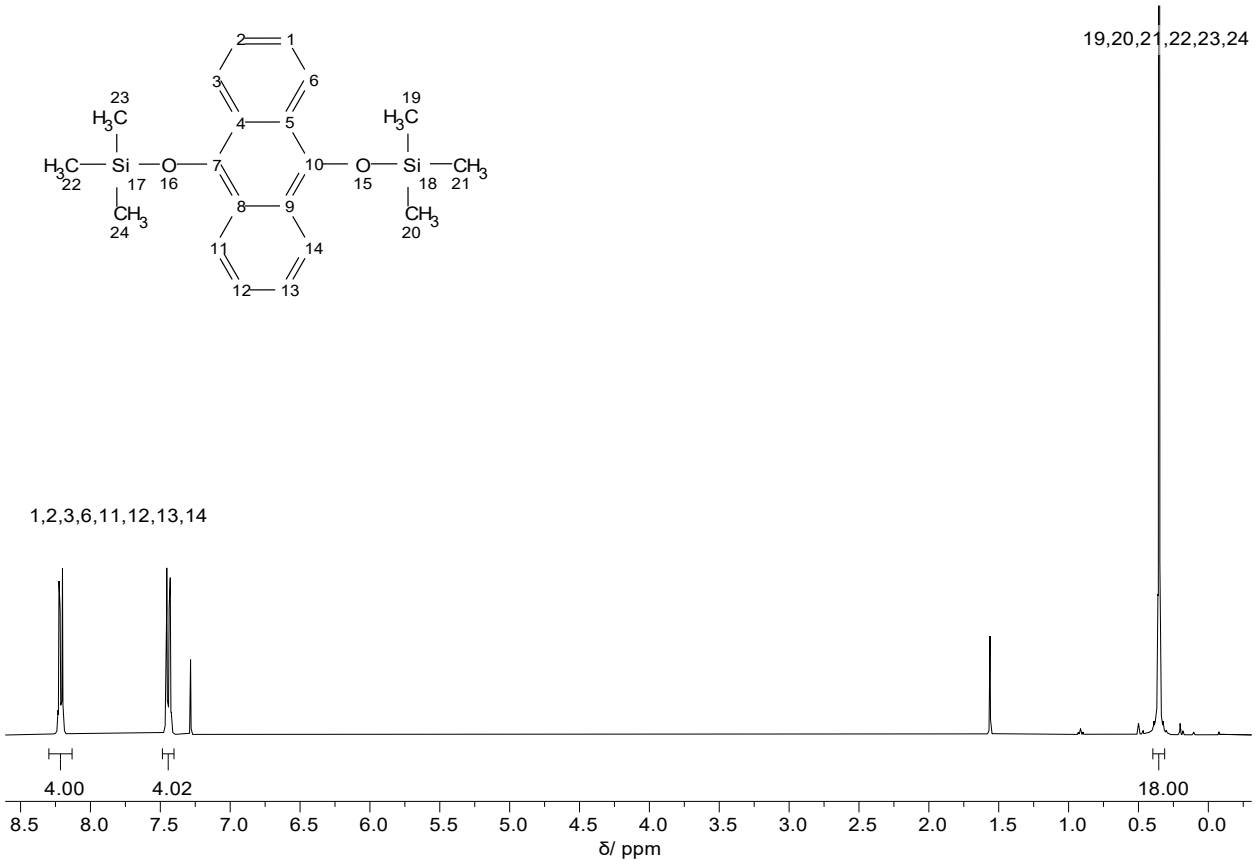

Figure S10. 400 MHz ^{1}H NMR spectrum in $CDCl_3$ of **7**

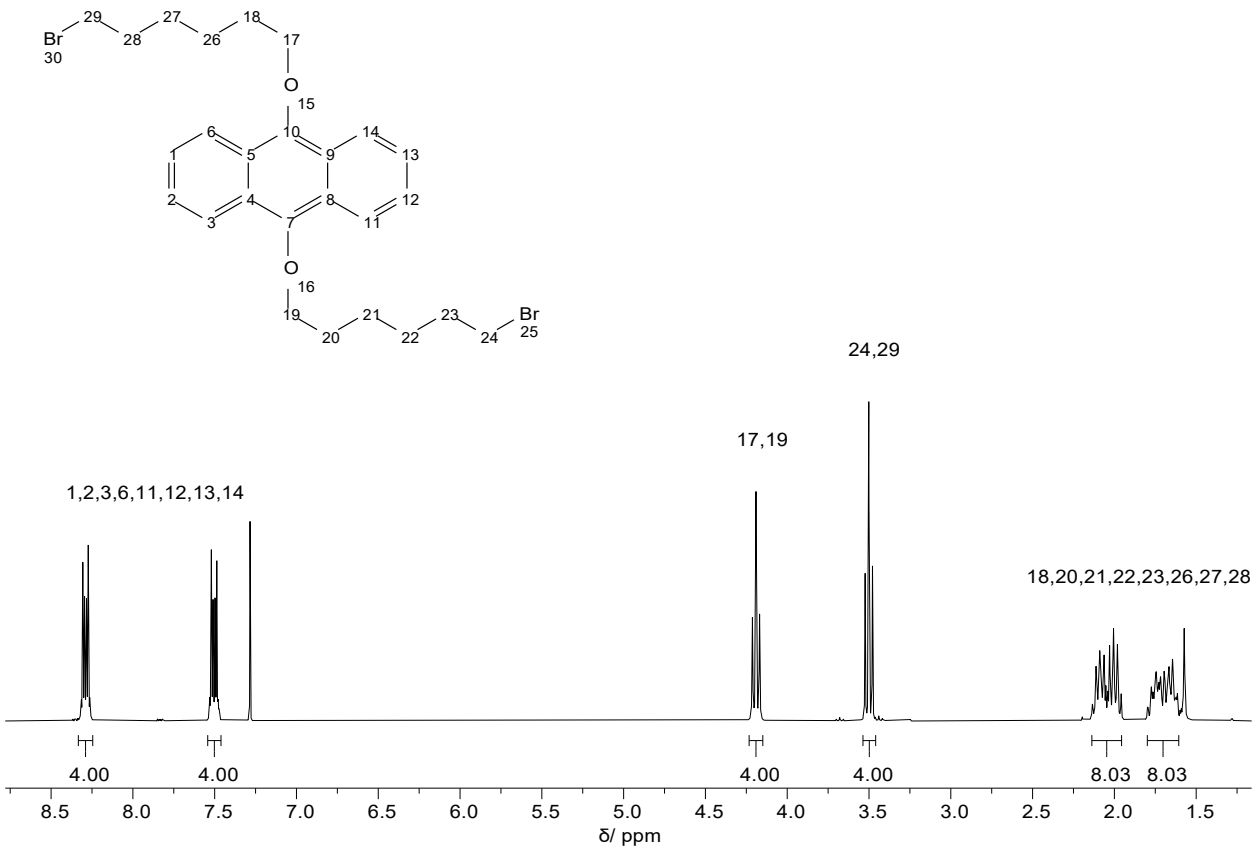

Figure S11. 300 MHz ^{1}H NMR spectrum in $CDCl_3$ of **8**

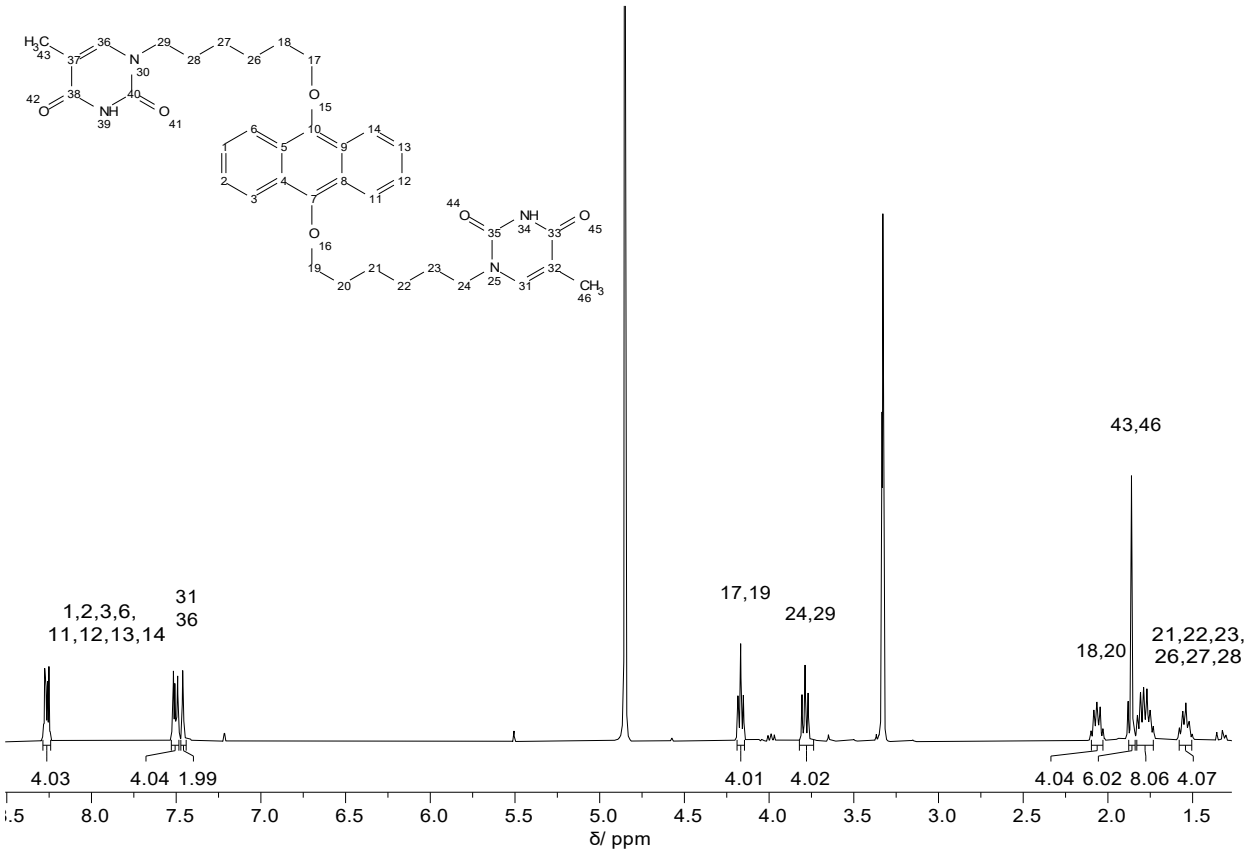

Figure S12. 400 MHz ^{1}H NMR spectrum in CD_3OD of **Th-An-Th**

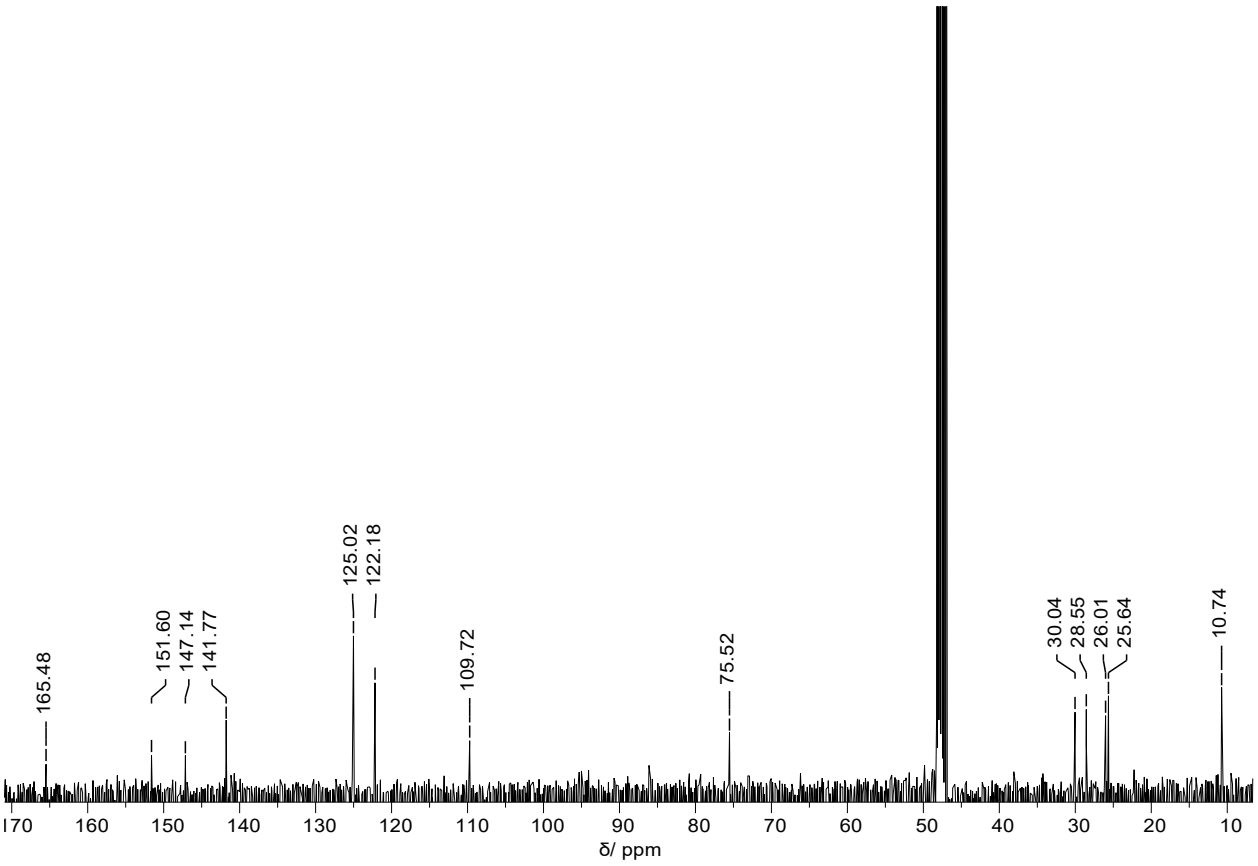

Figure S13. 101 MHz ^{13}C NMR spectrum in CD_3OD of **Th-An-Th**

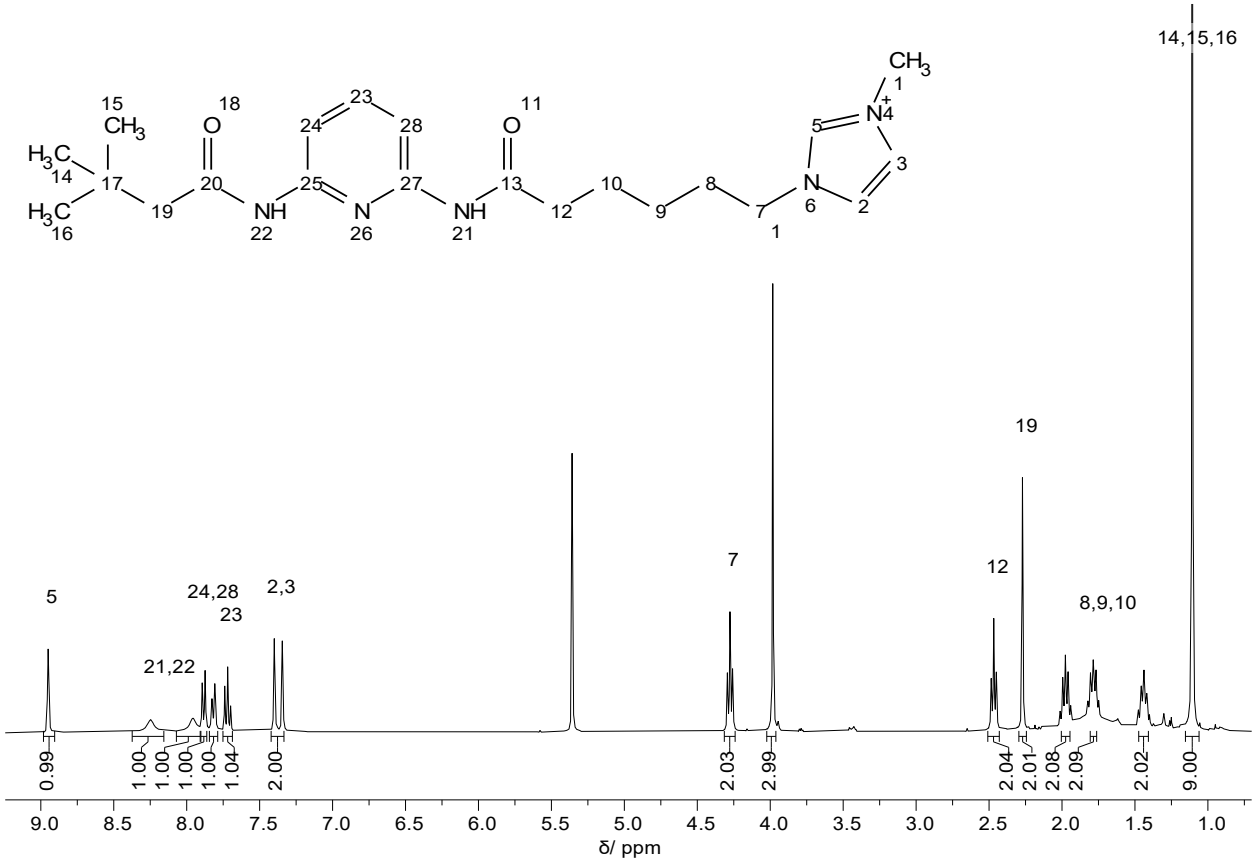

Figure S14. 400 MHz ^{1}H NMR spectrum in CD_2Cl_2 of **$(DAPIm)_2Mo_6$**

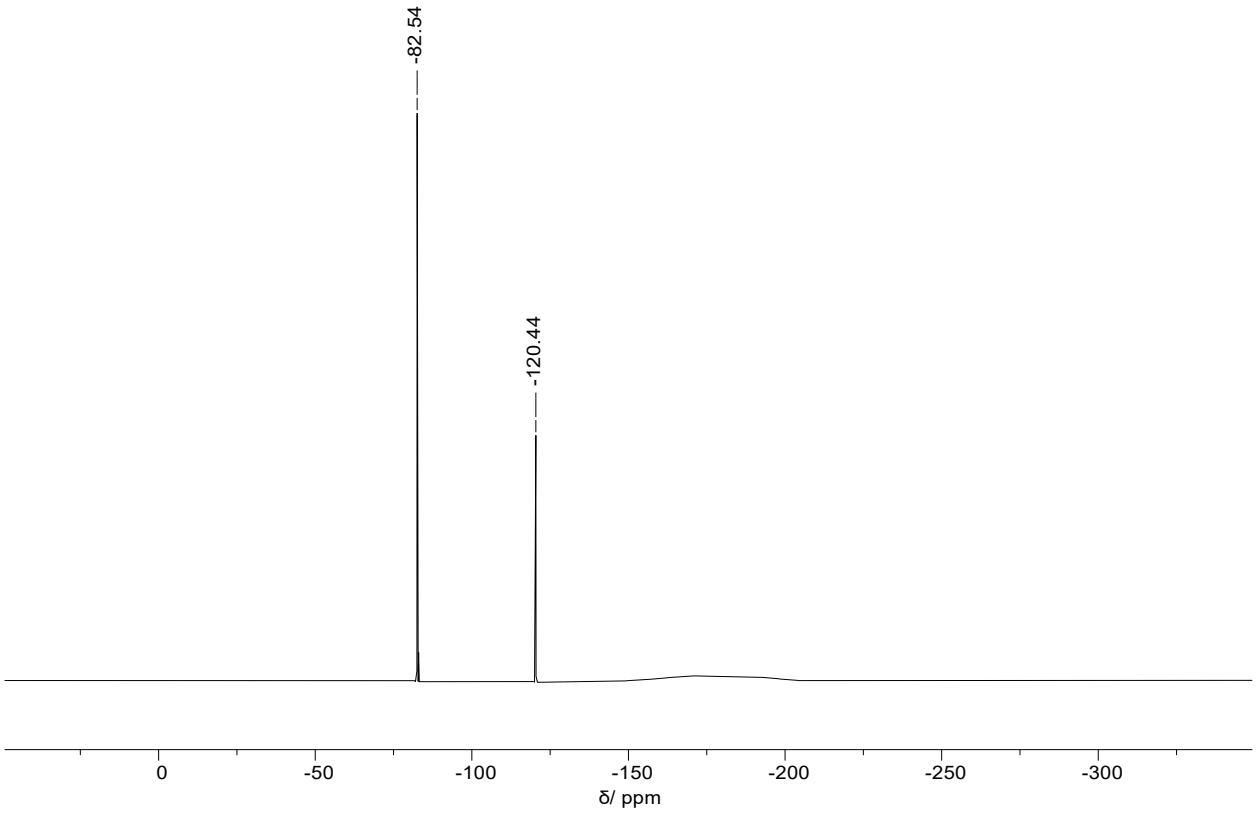

Figure S15. 376 MHz ^{19}F NMR spectrum in CD_2Cl_2 of **$(DAPIm)_2Mo_6$**

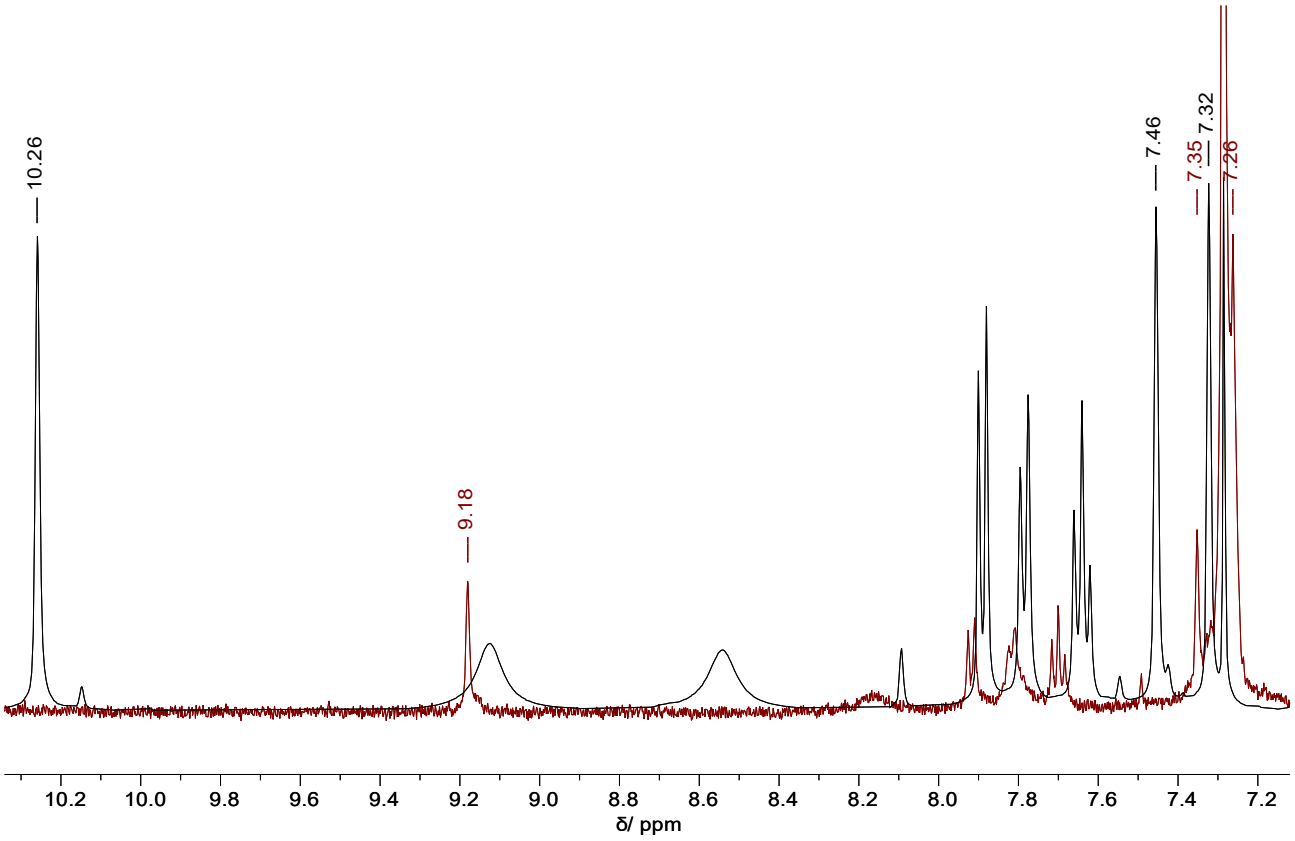

Figure S16. Comparison of ^1H NMR spectra in $CDCl_3$ of **DAPImBr** (black line, C = $4.3 \cdot 10^{-5}$M) and **$(DAPIm)_2Mo_6$** (red line, C = $4.5 \cdot 10^{-6}$M)

2. Binding constant determination

2.1. Binding constant for DAPImBr and An-Th

Table S1. NMR titration data for determination of binding constant in $CDCl_3$ between **DAPImBr** and **An-Th**

№	[$DAPIm^+$], M	[An-Th], M	[An-Th]/[$DAPIm^+$]	NH-1, ppm	NH-2, ppm	K, M^{-1}
1	$9.86 \cdot 10^{-4}$	0	0	8.32	8.98	
2	$9.86 \cdot 10^{-4}$	$9.77 \cdot 10^{-4}$	0.99	8.66	9.23	
3	$9.86 \cdot 10^{-4}$	$1.91 \cdot 10^{-3}$	1.94	8.91	9.40	
4	$9.86 \cdot 10^{-4}$	$2.79 \cdot 10^{-3}$	2.83	9.09	9.52	
5	$9.86 \cdot 10^{-4}$	$3.64 \cdot 10^{-3}$	3.69	9.23	9.61	
6	$9.86 \cdot 10^{-4}$	$4.45 \cdot 10^{-3}$	4.51	9.33	9.68	**261±2**
7	$9.86 \cdot 10^{-4}$	$5.23 \cdot 10^{-3}$	5.30	9.42	9.74	
8	$9.86 \cdot 10^{-4}$	$6.68 \cdot 10^{-3}$	6.77	9.55	9.82	
9	$9.86 \cdot 10^{-4}$	$8.01 \cdot 10^{-3}$	8.12	9.64	9.89	
10	$9.86 \cdot 10^{-4}$	$9.24 \cdot 10^{-3}$	9.37	9.70	9.93	
11	$9.86 \cdot 10^{-4}$	$1.09 \cdot 10^{-2}$	11.05	9.78	9.98	

2.2. Binding constant for $(DAPIm)_2Mo_6$ and An-Th

Table S2. NMR titration data for determination of binding constant in $CDCl_3$ between **$(DAPIm)_2Mo_6$** and **An-Th**

№	[$DAPIm^+$], M	[An-Th], M	[An-Th]/[$DAPIm^+$]	NH-1, ppm	NH-2, ppm	K, M^{-1}
1	$1.03 \cdot 10^{-3}$	0	0	7.81	8.17	
2	$1.03 \cdot 10^{-3}$	$9.39 \cdot 10^{-4}$	0.91	8.36	8.68	
3	$1.03 \cdot 10^{-3}$	$1.83 \cdot 10^{-3}$	1.78	8.74	9.01	
4	$1.03 \cdot 10^{-3}$	$2.69 \cdot 10^{-3}$	2.61	9.00	9.23	
5	$1.03 \cdot 10^{-3}$	$3.50 \cdot 10^{-3}$	3.40	9.18	9.40	
6	$1.03 \cdot 10^{-3}$	$4.23 \cdot 10^{-3}$	4.11	9.31	9.52	
7	$1.03 \cdot 10^{-3}$	$5.02 \cdot 10^{-3}$	4.87	9.42	9.61	**420±3**
8	$1.03 \cdot 10^{-3}$	$6.42 \cdot 10^{-3}$	6.23	9.56	9.74	
9	$1.03 \cdot 10^{-3}$	$7.70 \cdot 10^{-3}$	7.48	9.66	9.83	
10	$1.03 \cdot 10^{-3}$	$8.88 \cdot 10^{-3}$	8.62	9.73	9.89	
11	$1.03 \cdot 10^{-3}$	$9.98 \cdot 10^{-3}$	9.69	9.78	9.93	
12	$1.03 \cdot 10^{-3}$	$1.24 \cdot 10^{-2}$	12.04	9.87	10.00	

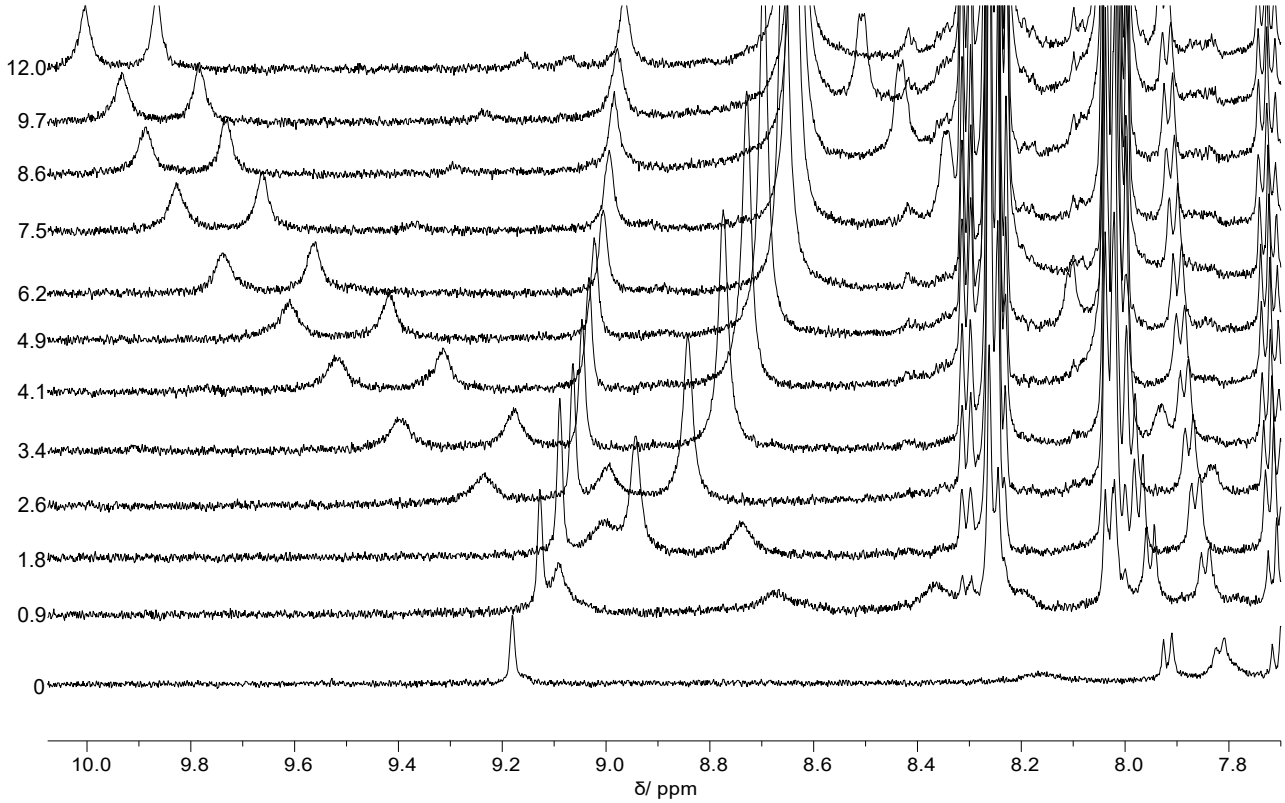

Figure S17. 500 MHz ^{1}H NMR spectra in $CDCl_3$ in the titration experiment with **$(DAPIm)_2Mo_6$** ($C = 1.03 \cdot 10^{-3}$M) and **An-Th** (values on the left are referred to the [**An-Th**]/[**$DAPIm^+$**] ratio)

2.3. Evidence of binding between $(DAPIm)_2Mo_6$ and Th-An-Th

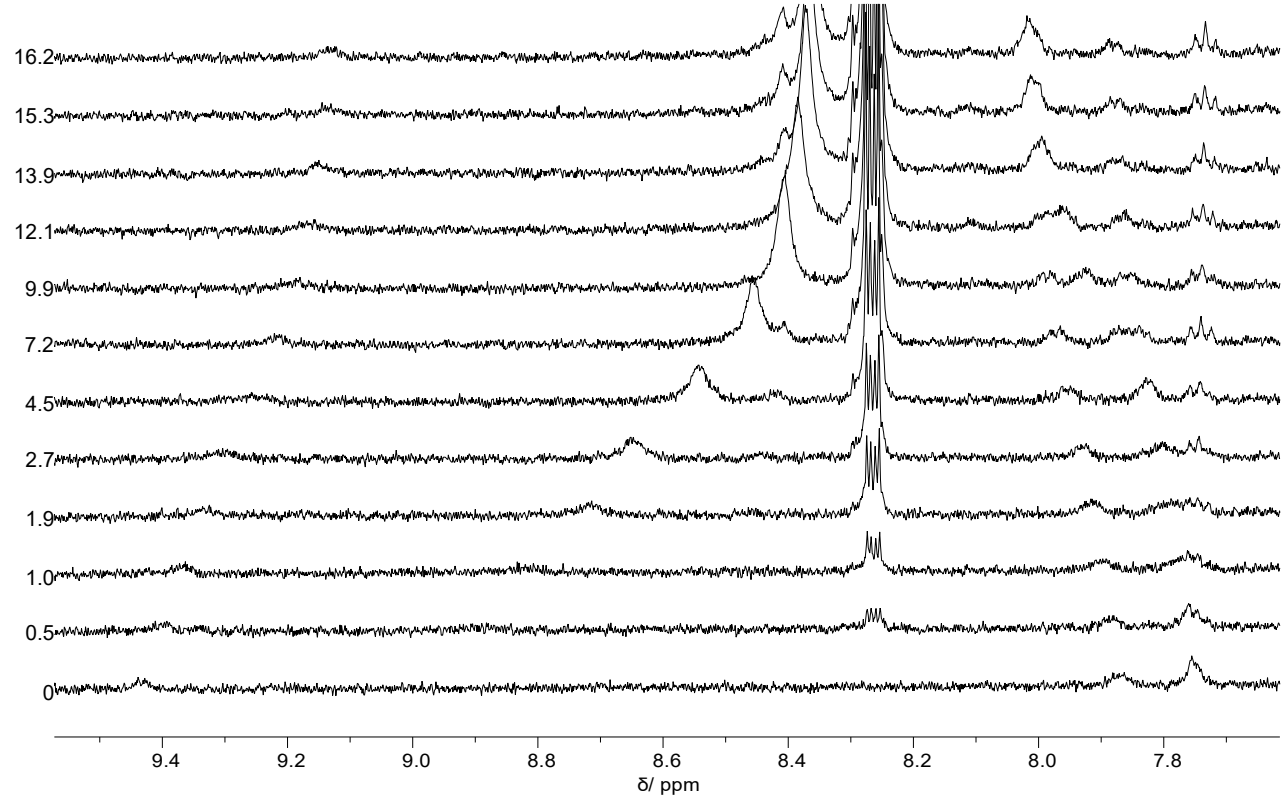

Figure S18. 500 MHz ^{1}H NMR spectra in $CDCl_3$ in the titration experiment with **$(DAPIm)_2Mo_6$** ($C = 9.07 \cdot 10^{-5}$M) and **Th-An-Th** (values on the left are referred to the [**Th-An-Th**]/[**$DAPIm^+$**] ratio)

3. Absorption spectra

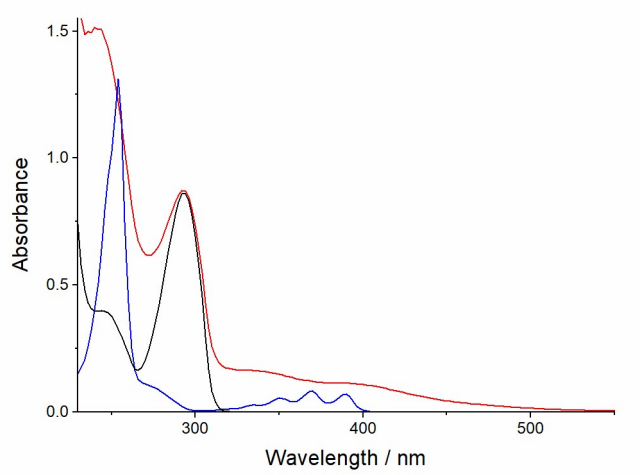

Figure S19. Absorption spectra in CH_3CN of **DAPImBr** (black line), **An-Th** (blue line) and **$(DAPIm)_2Mo_6$** (red)

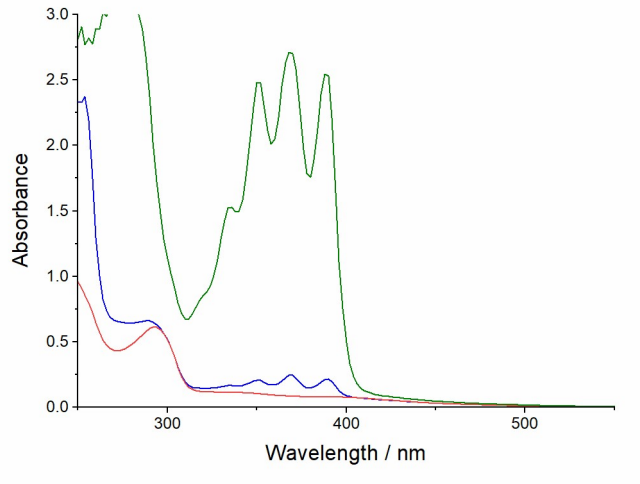

Figure S20. Absorption spectra in CH_3CN of $DAPIm_2Mo_6$ (red) + 1 equiv An-Th (blue) + excess of AnTh (green)

4. Emission decay profiles

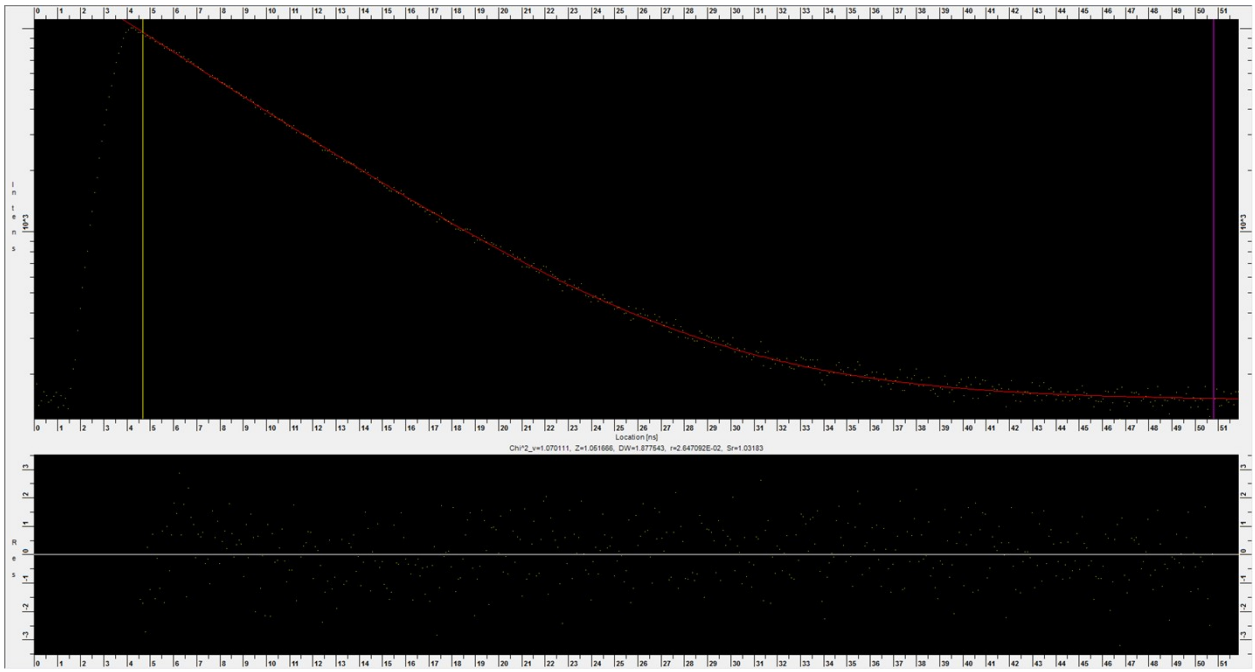

Figure S21. Emission decay profile of **An-Th** in $CHCl_3$ (λ_{ex} = 375 nm)

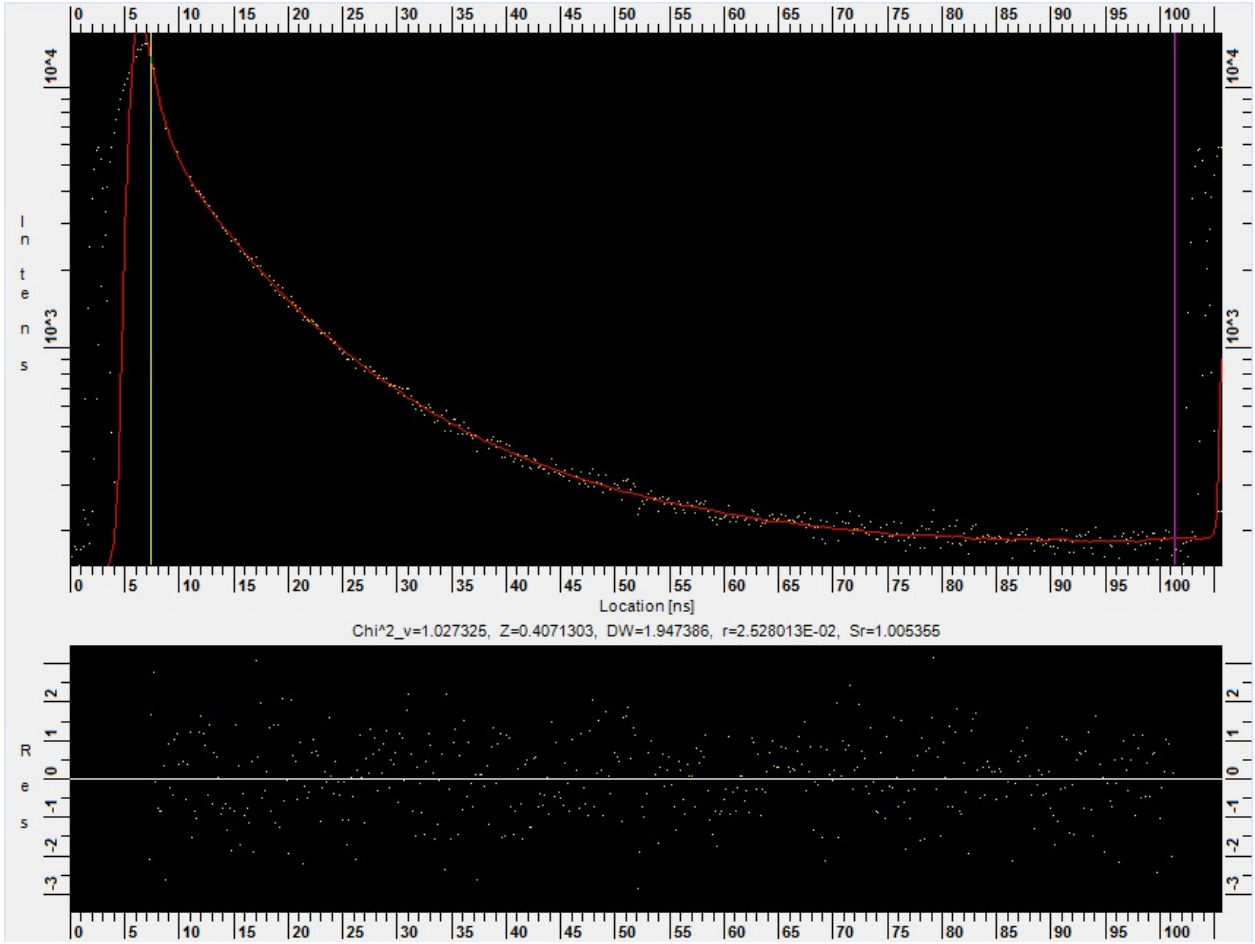

Figure S22. Emission decay profile of **Th-An-Th** in solid (λ_{ex} = 375 nm)

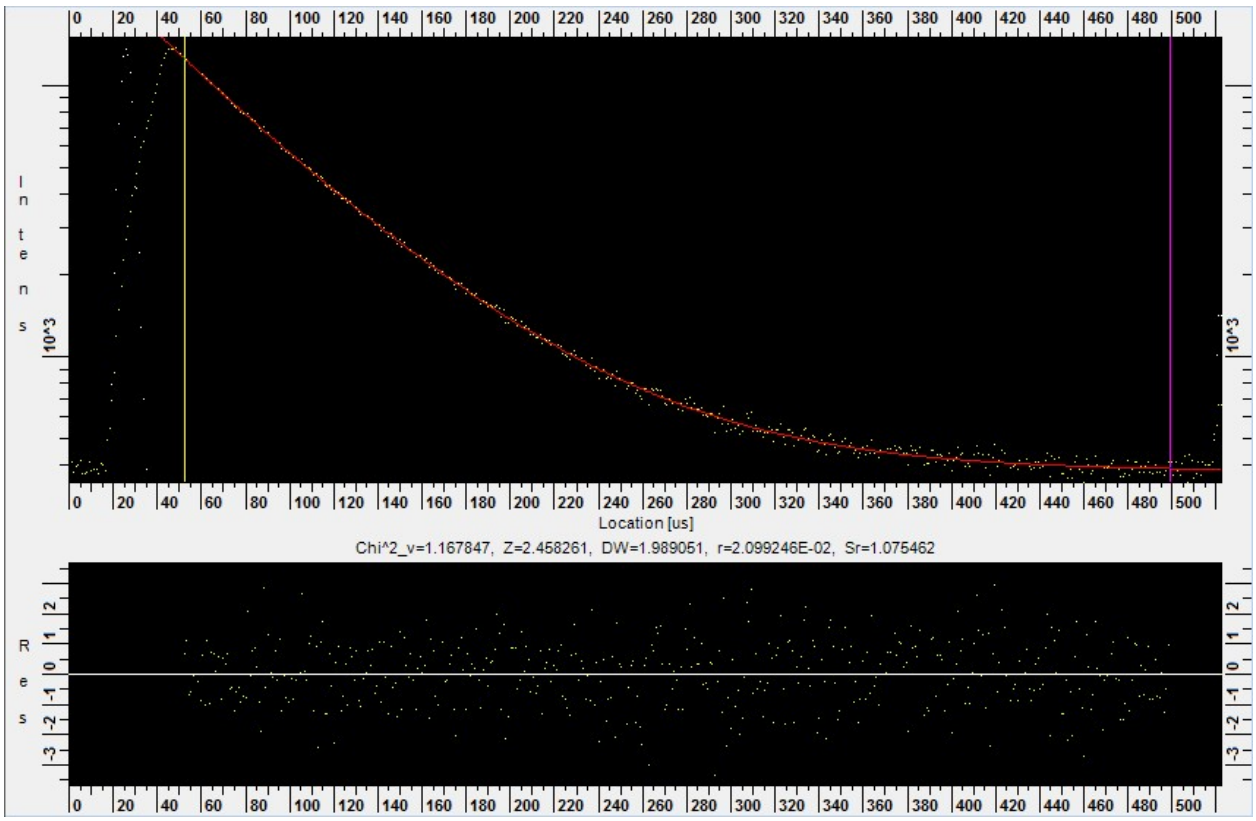

Figure S23. Emission decay profile of **$(DAPIm)_2Mo_6$** in deaerated (Ar) $CHCl_3$ (λ_{ex} = 375 nm)

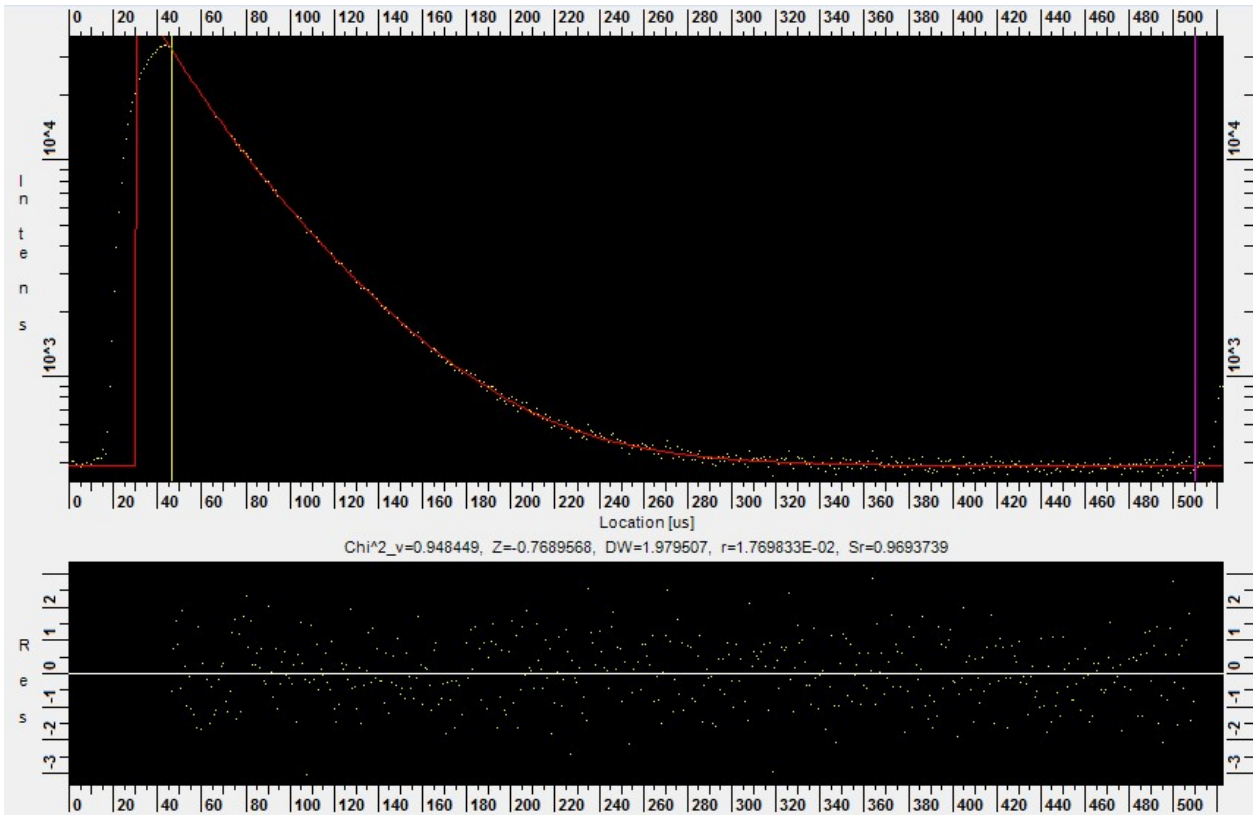

Figure S24. Emission decay profile of **$(DAPIm)_2Mo_6$** in solid (λ_{ex} = 375 nm)

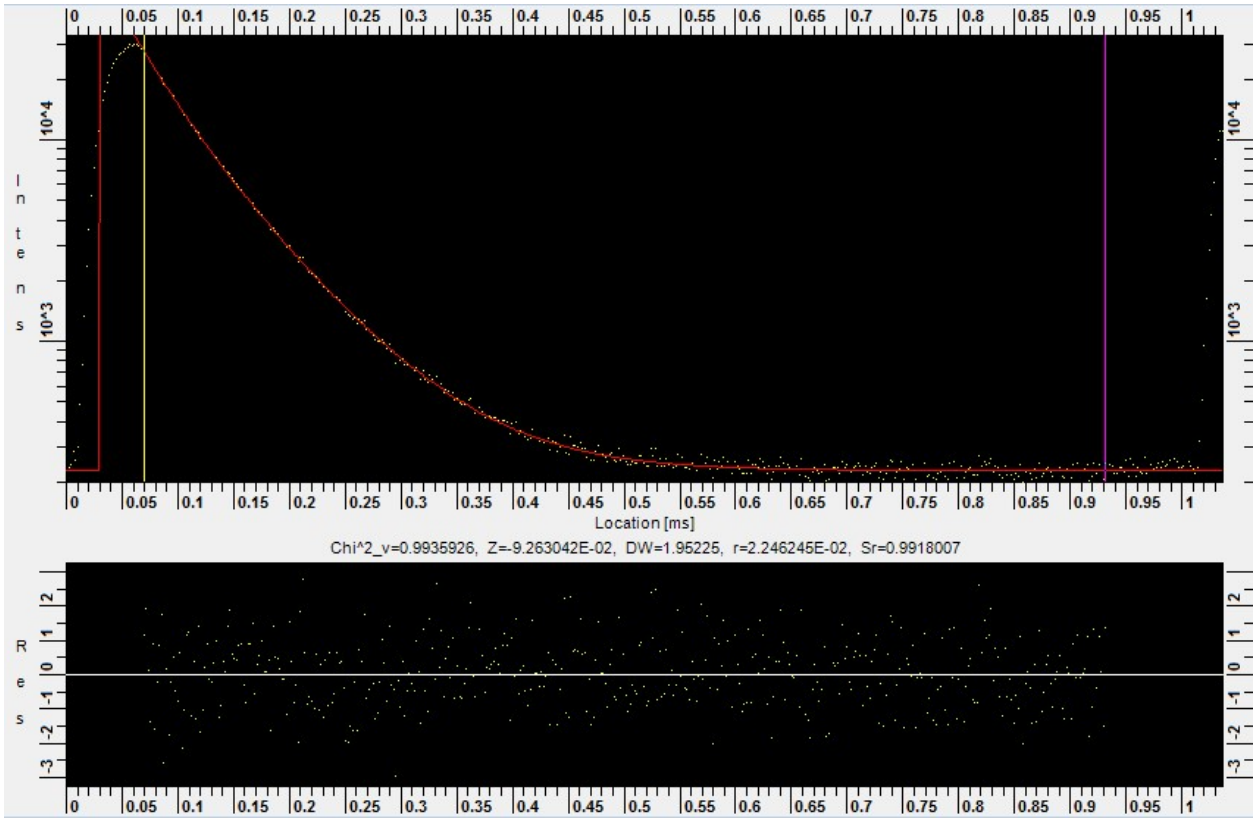

Figure S25. Emission decay profile of solid **(An-Th:DAPIm)$_2$Mo$_6$** (λ_{ex} = 375 nm)

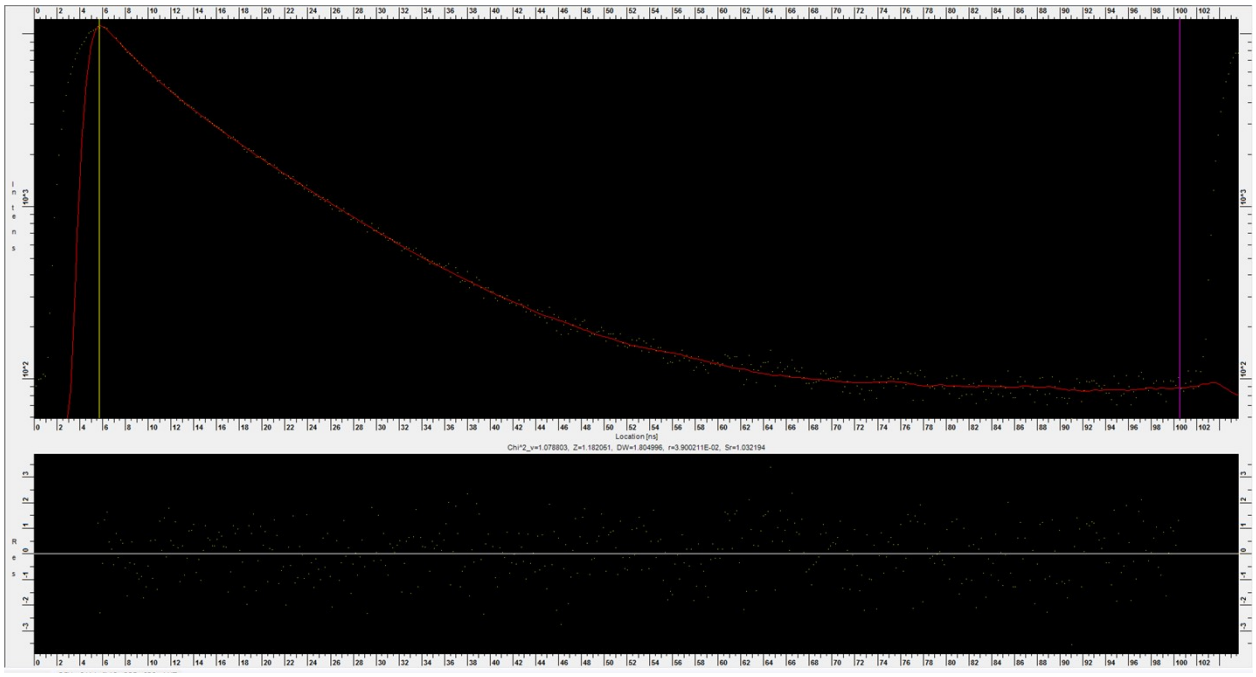

Figure S26. Emission decay profile of **Th-An-Th** in PMMA (λ_{ex} = 375 nm)

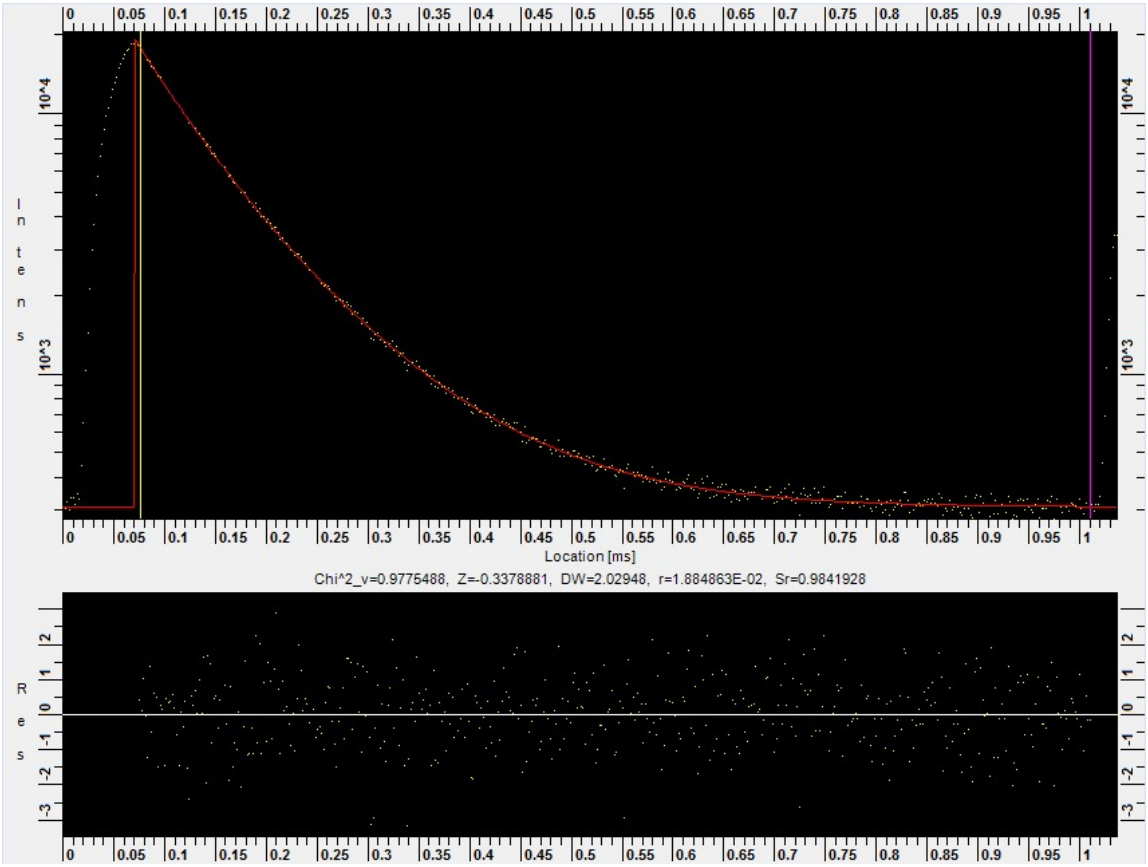

Figure S27. Emission decay profile of **$(DAPIm)_2Mo_6$** in PMMA (λ_{ex} = 375 nm)

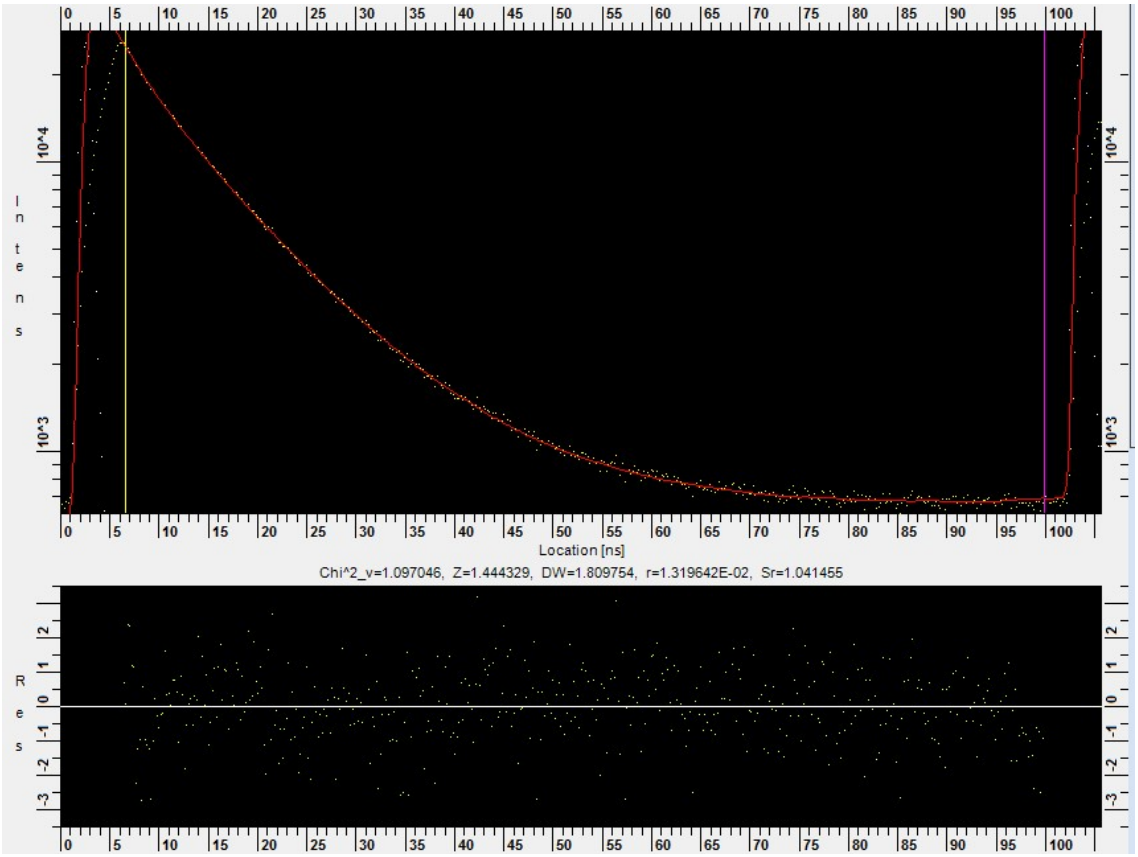

Figure S28. Emission decay profile of **Th-An-Th:$(DAPIm)_2Mo_6$** in PMMA (λ_{ex} = 375 nm, **Th-An-Th** component)

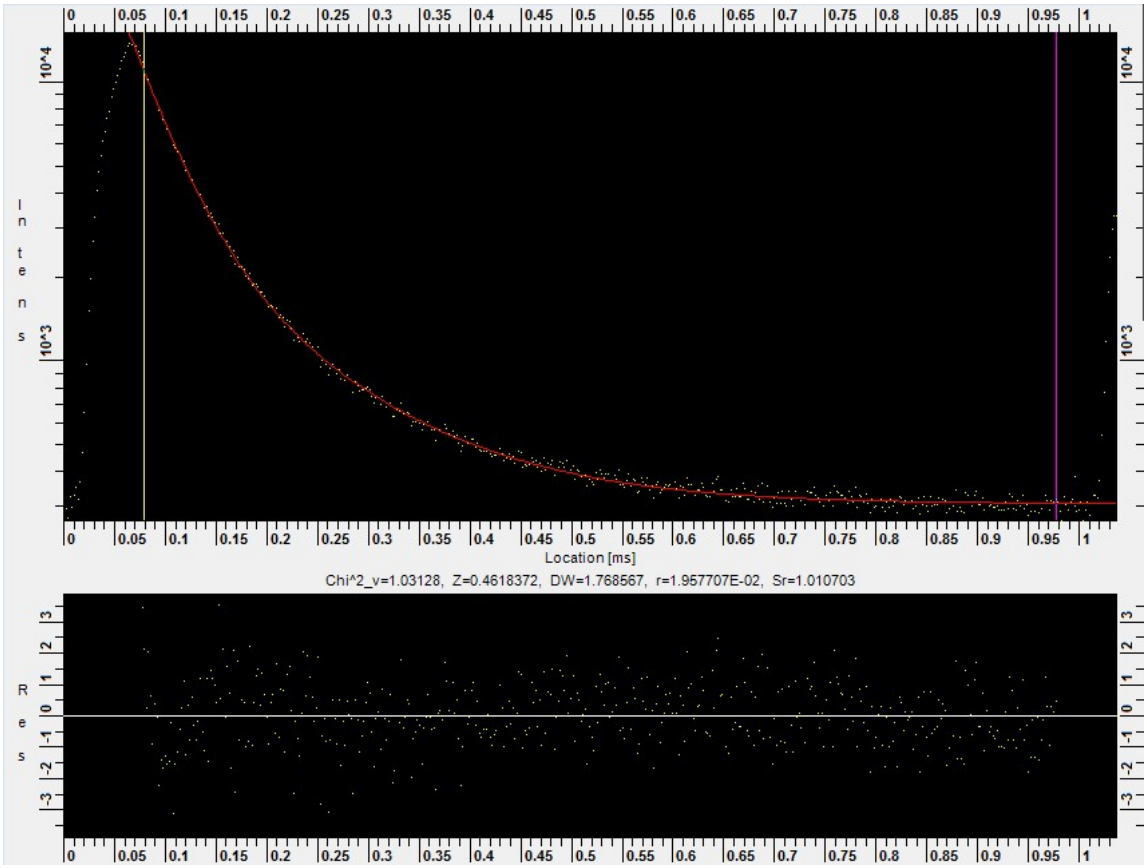

Figure S29. Emission decay profile of **Th-An-Th:(DAPIm)$_2$Mo$_6$** in PMMA (λ_{ex} = 375 nm, **Mo$_6$** component)

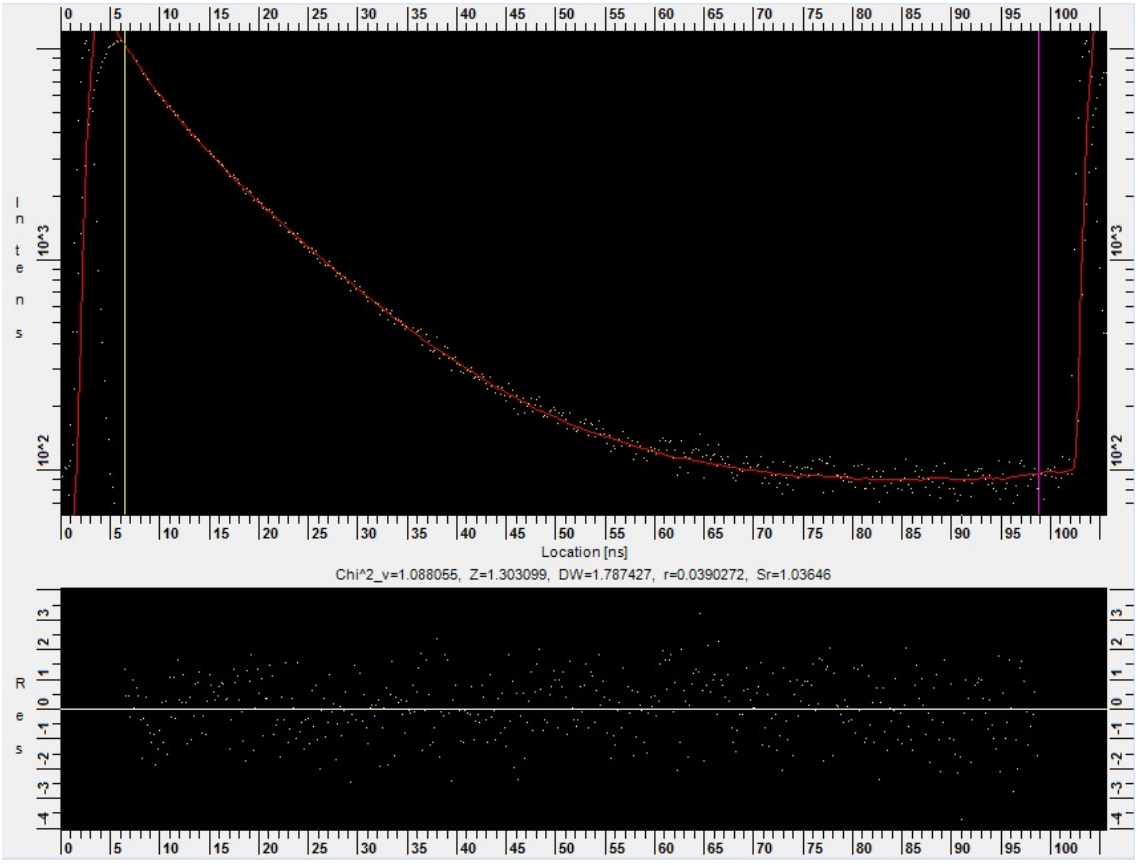

Figure S30. Emission decay profile of **Th-An-Th:(DAPIm)$_2$Mo$_6$** in PMMA in vacuum (λ_{ex} = 375 nm, **Th-An-Th** component**)**

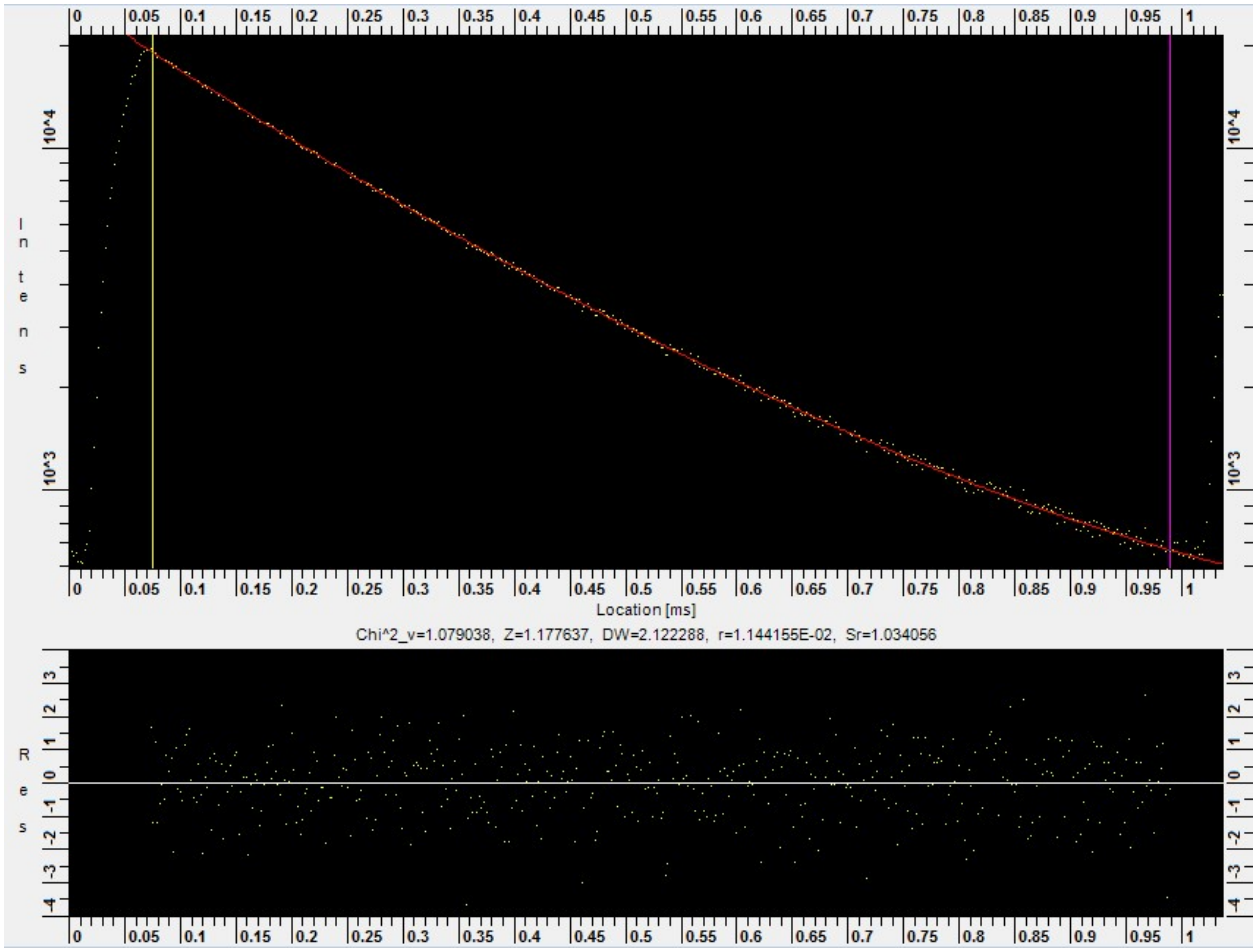

Figure S31. Emission decay profile of **Th-An-Th:(DAPIm)$_2$Mo$_6$** in PMMA in vacuum (λ_{ex} = 375 nm, **Mo$_6$** component)

5. Emission spectra

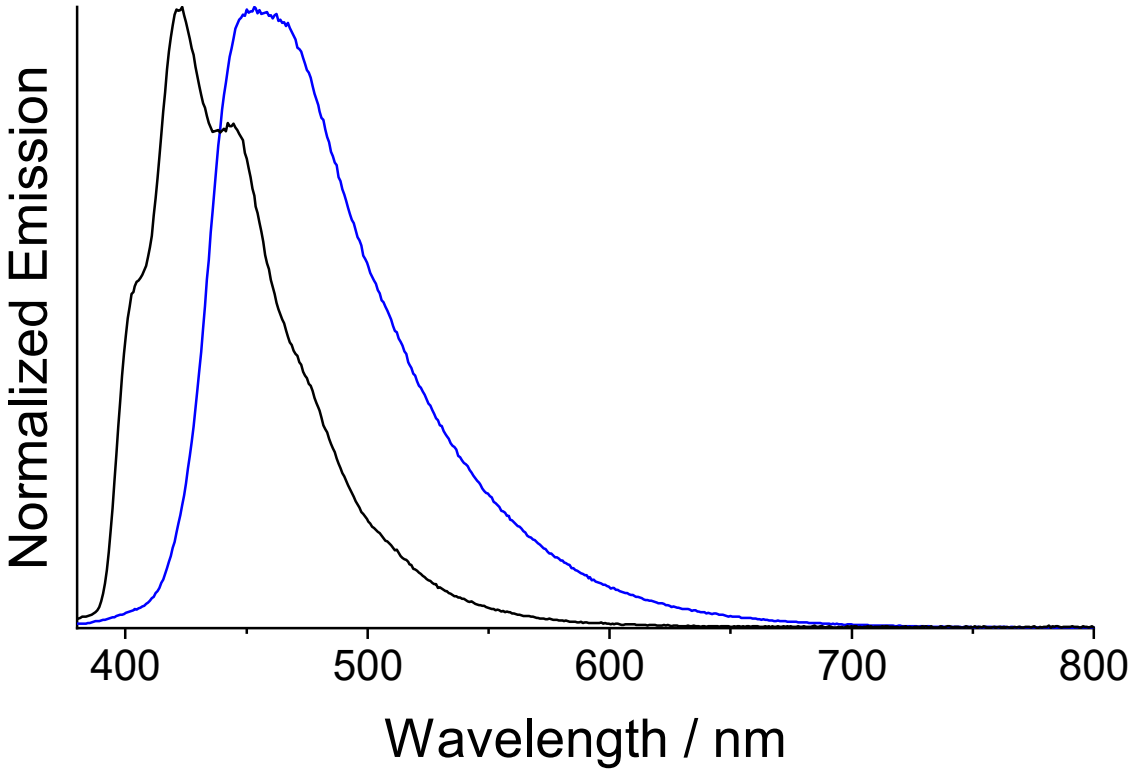

Figure S32. Emission spectra (λ_{ex} = 375 nm) of **An-Th (black line)** and **Th-An-Th (blue line)** in solid state

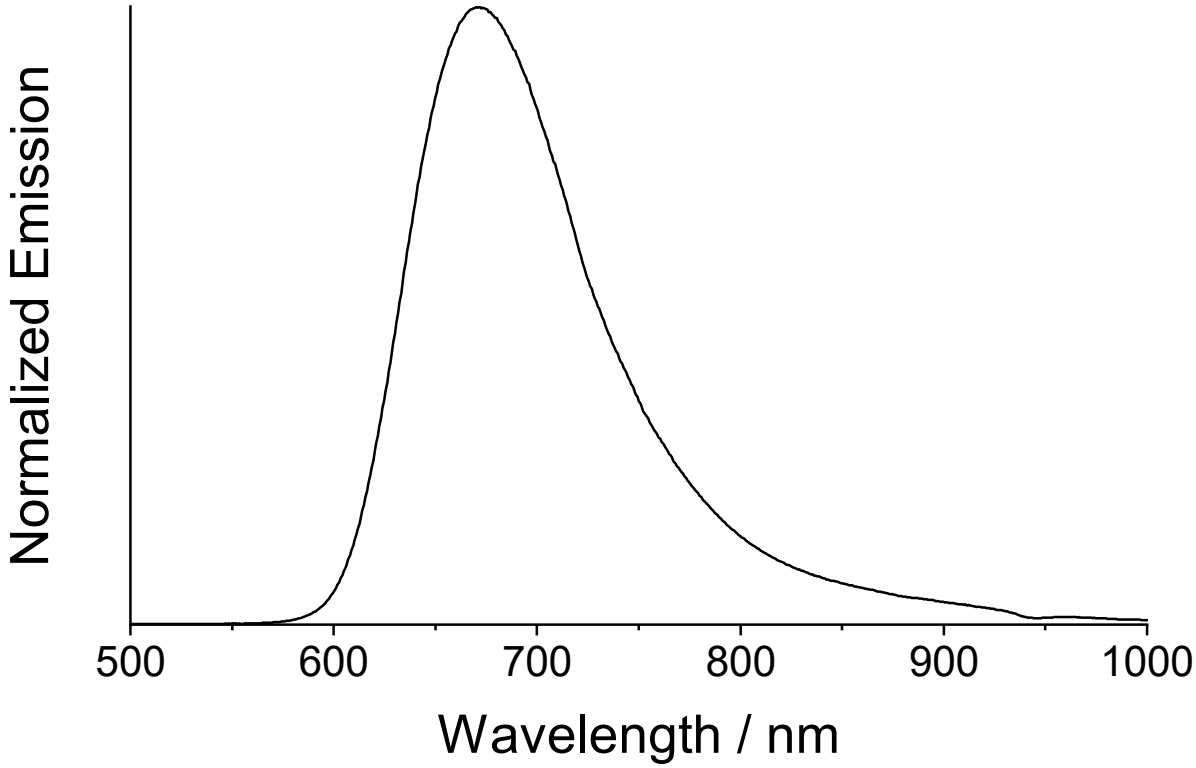

Figure S33. Emission spectrum (λ_{ex} = 375 nm) of **$(DAPIm)_2Mo_6$** in solid state

6. Förster radius determination

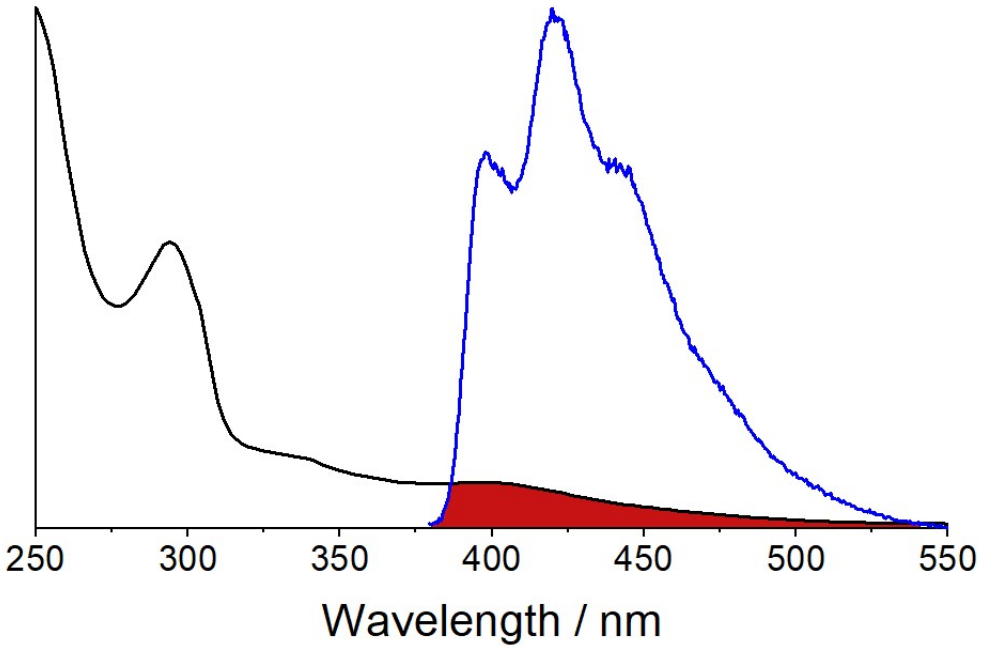

Figure S34. Representation of crossing of absorption spectrum of **$(DAPIm)_2Mo_6$** in $CHCl_3$ and emission spectrum of **An-Th** in $CHCl_3$

The following Forster rate equation describes the energy transfer by dipolar interaction:

$$k = \frac{1}{\tau_D}(\frac{R_0}{r})^6, R_0^6 = 8.785 \times 10^{-5}\frac{K^2\Phi_D J}{n^4}$$

Where τ_D is the donor lifetime in the absence of acceptor, *r* is the donor-acceptor distance, and R_0 is the Förster distance at which the energy transfer rate is equal to the decay rate. The Förster distance is related to the orientation factor, K^2 between donor and acceptor, and the donor and acceptor spectroscopic properties. *K* was taken as 2/3 that is appropriate for dynamic random orientation averaging of the donor and acceptor. Φ_D is the quantum yield of the donor in the absence of an acceptor (0.44 for An-Th). The index of refraction, n, is the index of refraction of $CHCl_3$: 1.4458. *J* is the overlap integral between the donor and acceptor that is calculated using the following equation:

$$J = \int_0^{+\infty} F_D(\lambda)\varepsilon_A(\lambda)\lambda^4 d\lambda$$

Where F_D is the area-normalized fluorescence spectrum of the donor,[1] ε_A is the molar absorption coefficient of the acceptor. The scaling constant is set such that when ε is in units of $M^{-1}.cm^{-1}$ and wavelength in units of nm, the Förster distance is in units of Å.[2]

The Förster radius was evaluated at 298K.

7. Emission titration data

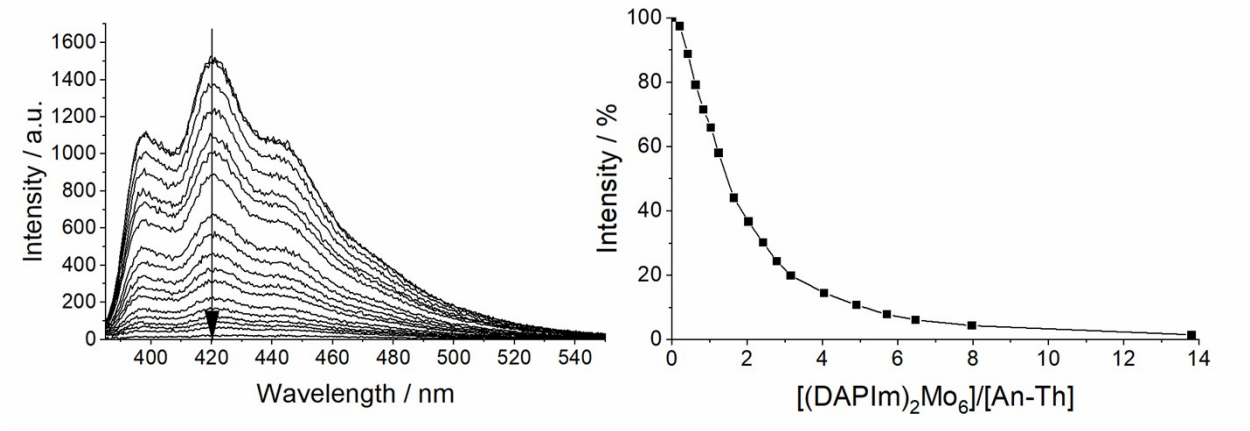

Figure S35. Emission spectra of **An-Th** (C = $1.23 \cdot 10^{-5}$M in $CHCl_3$) upon addition of aliquots of **$(DAPIm)_2Mo_6$**

Table S3. Anthracene excited state lifetime evolution ([An-Th] = $1.23 \cdot 10^{-5}$M) upon addition of **$(DAPIm)_2Mo_6$** in $CHCl_3$

[$(DAPIm)_2Mo_6$]/[An-Th]	τ_1, ns (A)	τ_2, ns (A)	τ_{av}, ns
0.4	5.8	-	5.8
0.7	10 (18 %)	5.1 (82 %)	6.6
1.8	7.9 (44 %)	3.7 (56 %)	6.3
3.4	8.3 (39 %)	3.8 (61 %)	6.4

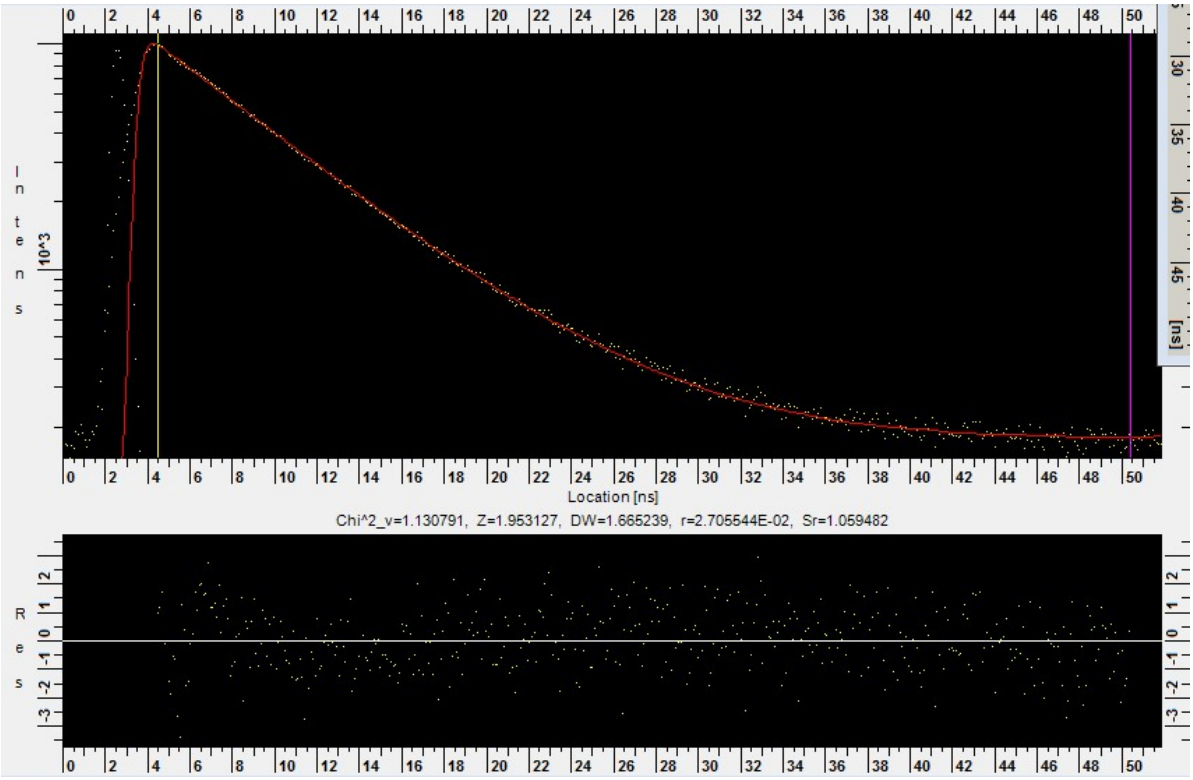

Figure S36. Emission decay profile of mixture of **$(DAPIm)_2Mo_6$** and **An-Th** in $CHCl_3$ ([**$(DAPIm)_2Mo_6$**]/[**An-Th**] = 0.4)

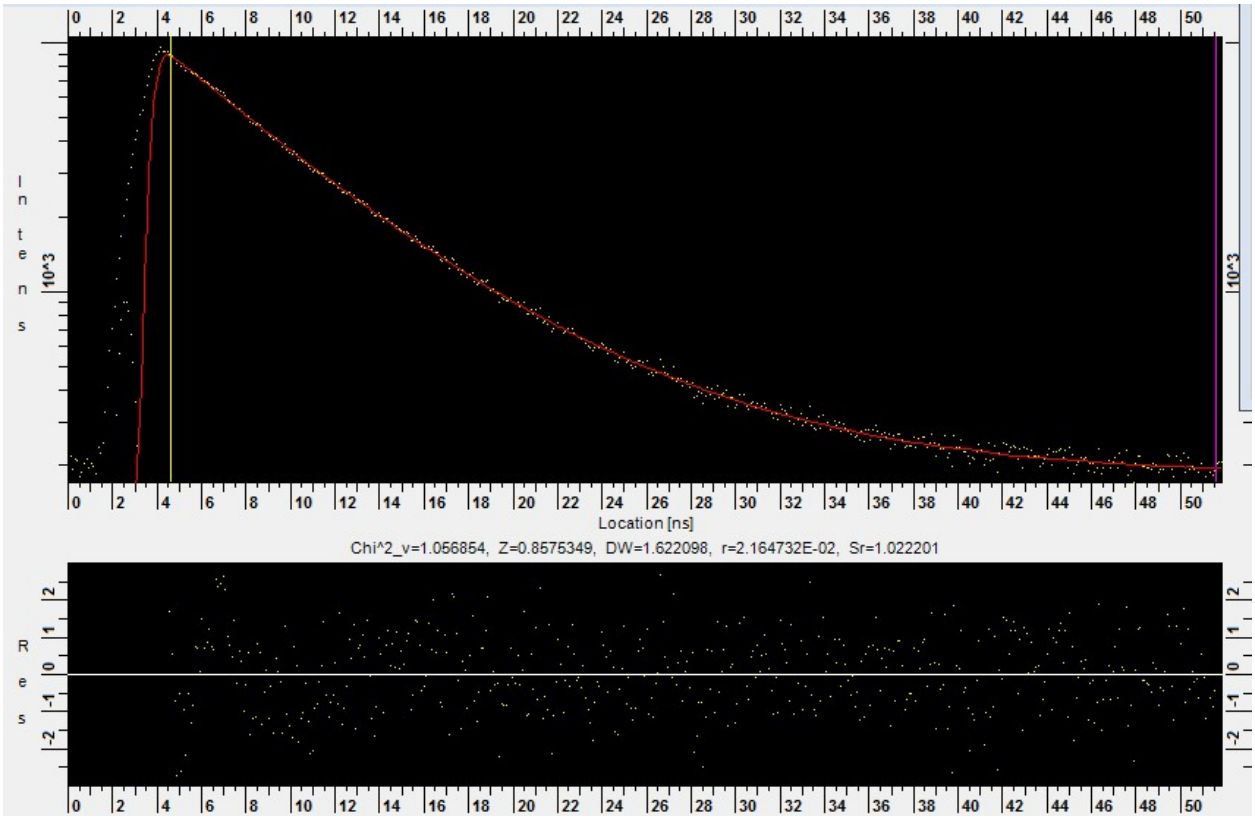

Figure S37. Emission decay profile of mixture of **$(DAPIm)_2Mo_6$** and **An-Th** in $CHCl_3$ ([**$(DAPIm)_2Mo_6$**]/[**An-Th**] = 0.7)

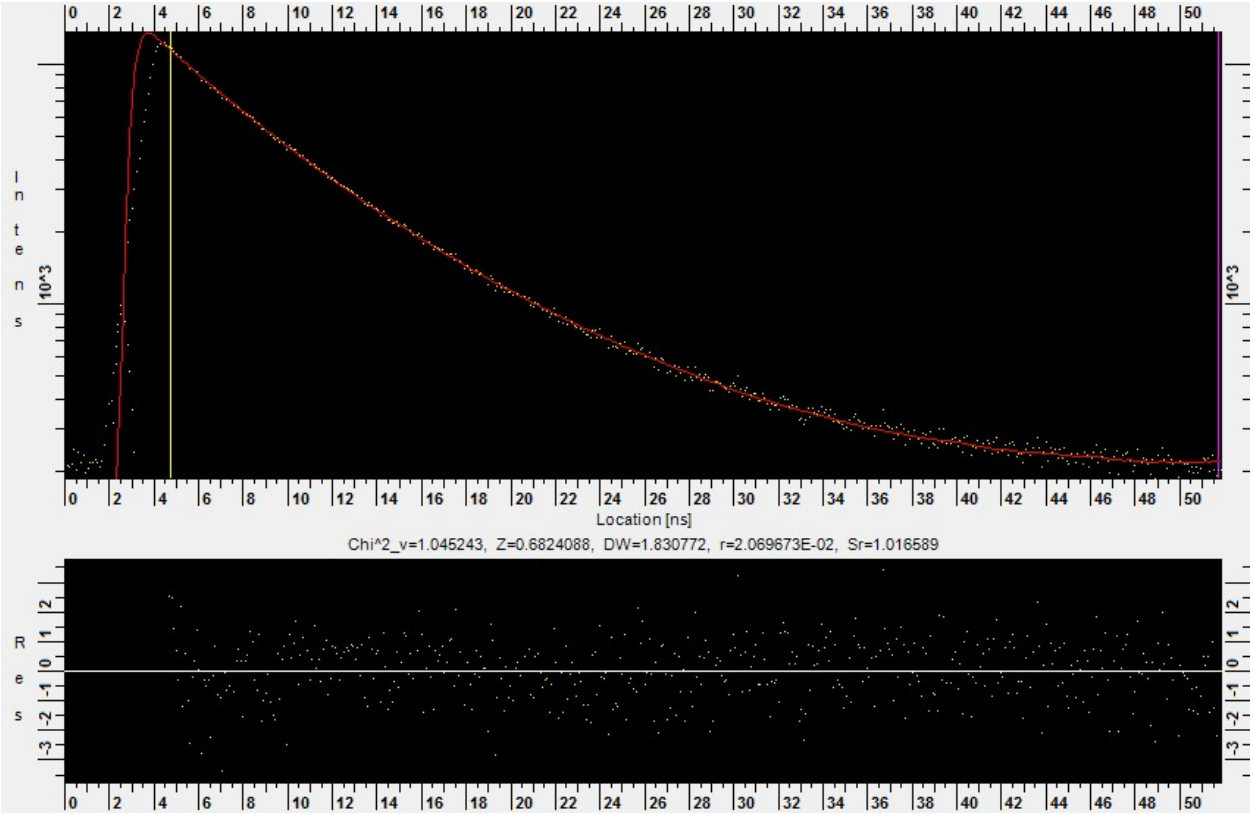

Figure S38. Emission decay profile of mixture of **$(DAPIm)_2Mo_6$** and **An-Th** in $CHCl_3$ ([**$(DAPIm)_2Mo_6$**]/[**An-Th**] = 1.8)

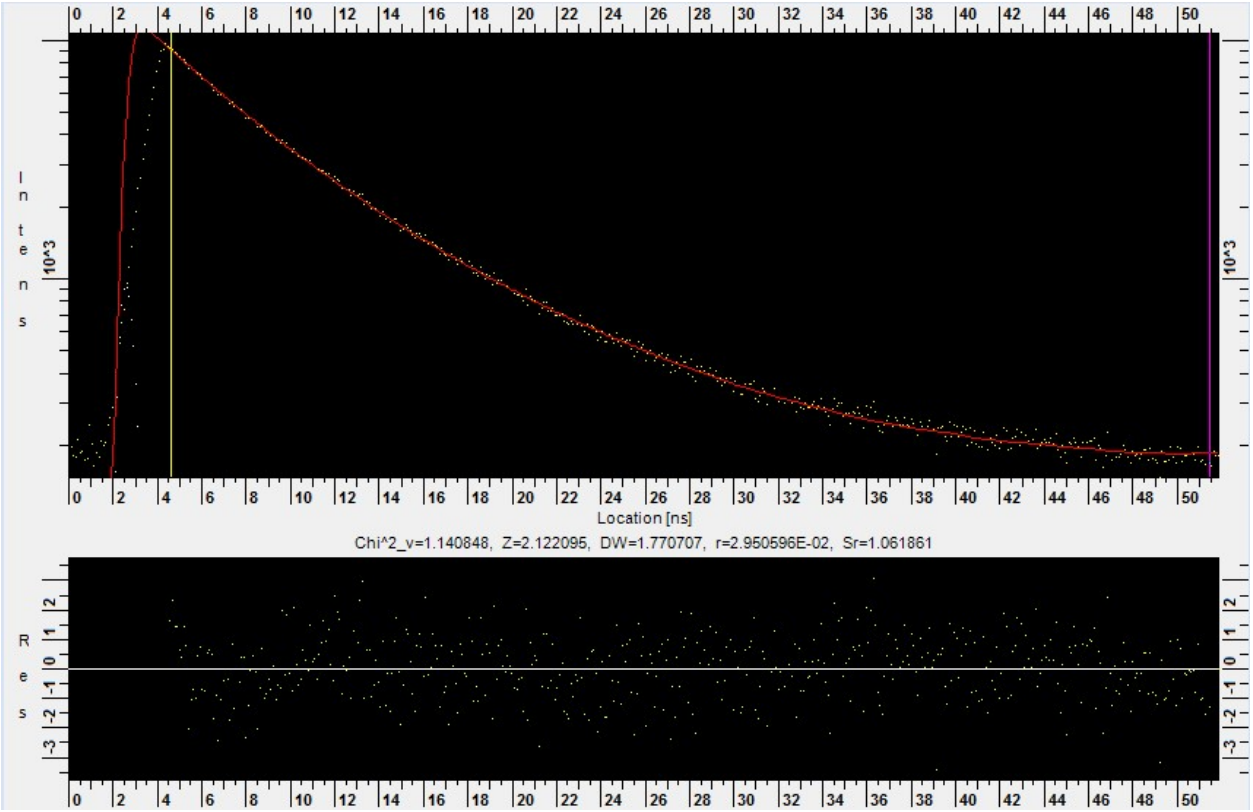

Figure S39. Emission decay profile of mixture of **$(DAPIm)_2Mo_6$** and **An-Th** in $CHCl_3$ ([**$(DAPIm)_2Mo_6$**]/[**An-Th**] = 3.4)

8. Emission evolution in vacuum

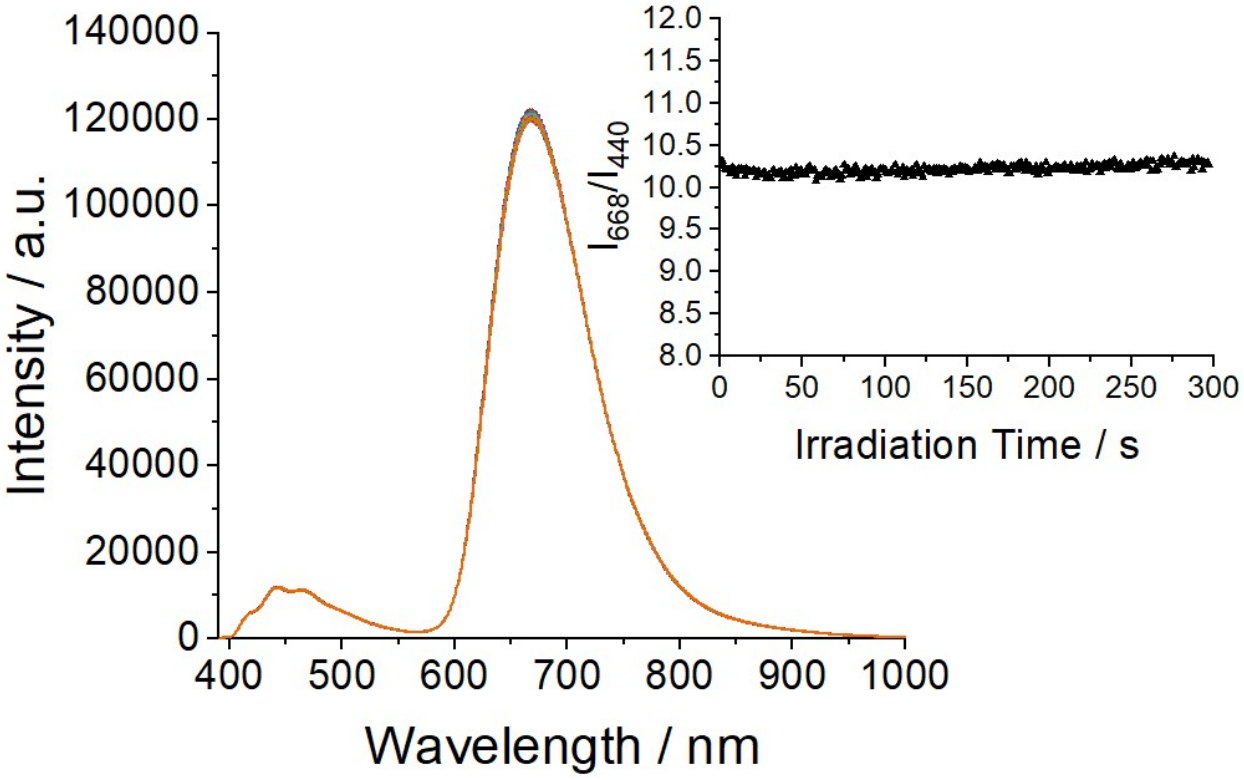

Figure S40. Evolution of emission spectra of **Th-An-Th:$(DAPIm)_2Mo_6$** under 5 min laser irradiation in vacuum (λ_{ex} = 375 nm, laser diode, 100 MHz, 100 ms int. time, $1.9 \cdot 10^{-6}$ hPa)

[1] J. R. Lakowicz, *Principles of Fluorescence Spectroscopy, third edition*, Springer, Boston, MA, **2006**.

[2] P. G. Wu, L. Brand, *Anal. Biochem.* **1994**, *218*, 1-13.